On the seasonal and mesoscale variabilities of the Northern Current during the PRIMO-0 experiment in the western Mediterranean Sea

Northern Current
Ligurian Sea
Flux
Variability
Meanders

Courant Nord
Mer Ligure
Flux
Variabilité
Méandres

Corinne ALBÉROLA [1], Claude MILLOT [1] and Jordi FONT [2]

[1] Centre d'Océanologie de Marseille, CNRS, BP 330, 83507 La Seyne/mer, France.

[2] Instituto de Ciencias del Mar, CSIC, P. Joan de Borbò, 08039 Barcelona, Spain.

ABSTRACT

In the western Mediterranean Sea, the Northern Current is one of the major veins and is formed by the junction, in the Ligurian Sea, of the currents flowing northward along each side of Corsica; it is recognized as an entity along the continental slope as far as the Catalan Sea, surrounding the central zone where dense water formation occurs in winter. The seasonal and mesoscale variabilities of the Northern Current are analysed from a fortnightly hydrological survey carried out off Nice to a distance of ~55 km, from October 1990 to July 1991, and from ~30 current time series collected as deep as 2000 m, on four moorings set within a ~30 km coastal band from December 1990 to May 1991, in the framework of the PRIMO-0 experiment. The hydrological surveys have mainly evidenced the spreading of Levantine Intermediate Water (LIW) in an on-offshore direction, the transformation of Modified Atlantic Water (MAW) into Winter Intermediate Water (WIW) in the deep winter, as well as the advection of less modified MAW. From a dynamic point of view, the seasonal variability is mainly depicted as a well-defined episode of narrowing, deepening and shoreward shift, from late January to mid-March, of a generally wide and shallow Northern Current. Currents have clearly appeared to be similar and highly correlated in an upper layer, the thickness of which is at least a hundred metres (between ~60 and 150 m), irrespective of the location of the points and of the season. This layer is expected to extend up to the surface. The flux of the Northern Current (between 0 and ~300 m) has ranged within 1-1.6 Sv from autum to summer, in agreement with the known values; relatively high values have been maintained during a rather long winter season. In accordance with other observations which have provided a description of a complete annual cycle, mesoscale activity is found to increase from autumn to deep winter and then displays a continuous decrease until summer at least. Mesoscale events have appeared to extend vertically over some few hundred metres, and the EOF decomposition has shown quasi no rotation of the fluctuations with depth. So, such events should have a relatively simple vertical structure, corresponding mainly to the first baroclinic mode with its zero-crossing at 400-500 m. Currents are relatively well represented by the barotropic and first baroclinic modes, the latter being predominant and more energetic, especially in winter. However, consequently to the variations of the Northern Current in width and depth, our most seaward point (~30 km) is either outside or more or less within this current, so that the dynamic regime is generally more complex there. Nevertheless, the observed mesoscale events become, in deep winter, the barotropic ones of the central zone governed by vigorous convection. The fluctuations have generally shorter time scales in winter than in spring. Due to dra-

matic winter transformations, the Northern Current is mainly observed to be altered by instability processes, leading to meanders. Indeed, an important finding, based on the standard deviation ellipses and spectral analysis, is that its major fluctuations clearly appear to be quasi transverse within its own core. Moreover, from the polarization of energy, the signature of steep and large mesoscale meanders is clearly evidenced at 10-20 days. These meanders have far greater energy in winter than in spring, when they have slightly shorter periods (~10 days). As previously observed, shorter fluctuations at 3-6 days with smaller amplitudes than those of the meanders at 10-20 days are also associated with a meandering current; they are expected to be intensified from spring-summer to the deep winter. In spring, while the flow is more stable, the predominant fluctuations resemble pulses of the current that may be expected to extend horizontally to a few tens of kilometres. Fundamental to coastal oceanographic problems is the fact that the circulation is actually unforeseeable in the coastal zone of ~10 km, where the main mesoscale phenomena have periods slightly shorter than in the core of the current. The major seasonal and mesoscale features of the Northern Current, especially the high flux values maintained during a relatively long winter season, *i.e.* during the period of dense water formation, its occasional narrowness and shoreward shift, and the extension of the central zone in deep winter, are probably very closely linked. Thus, as a hypothesis for further experimental and theoretical work, we suggest that the winter dense water formation should be effectively one of the major forcings of the circulation in the northern part of the western Mediterranean Sea.

RÉSUMÉ

Le courant Nord en mer Ligure.

En Méditerranée occidentale, l'une des principales veines est le courant Nord, formé par la jonction, en mer Ligure, des courants qui s'écoulent vers le Nord, de chaque côté de la Corse; il est reconnu comme une entité le long de la pente continentale jusqu'en mer Catalane, contournant la zone centrale où se forme l'eau dense en hiver. Les variabilités saisonnière et à méso-échelle sont analysées à la suite d'une surveillance hydrologique bimensuelle réalisée au large de Nice jusqu'à environ 55 km, d'octobre 1990 à juillet 1991, et à partir de près d'une trentaine de séries temporelles courantométriques collectées entre décembre 1990 et mai 1991 jusqu'à 2000 m de profondeur, sur quatre mouillages mis en place dans une bande côtière de 30 km, dans le cadre de l'expérience PRIMO-0. Cette surveillance a principalement mis en évidence, du point de vue hydrologique, les variations de la veine d'eau Levantine intermédiaire (LIW) dans la direction côte-large, la transformation d'eau Atlantique modifiée (MAW) en eau d'hiver intermédiaire (WIW) au cœur de l'hiver, et l'advection de MAW moins modifiée. Du point de vue dynamique, la variabilité saisonnière se traduit de fin janvier à mi-mars, par un épisode bien défini de rétrécissement, d'approfondissement et de rapprochement de la côte, du courant Nord qui, le reste du temps, est relativement large et peu profond. Les courants se sont révélés clairement similaires et fortement corrélés dans une couche supérieure d'au moins une centaine de mètres (entre environ 60 et 150 m), quelles que soient la position des points et la saison. Cette couche supérieure s'étend probablement jusqu'à la surface. Le flux du courant Nord (entre 0 et 300 m) varie entre 1 et 1,6 Sv de l'automne à l'été, en bon accord avec les valeurs publiées, et sa valeur reste relativement élevée pendant une saison hivernale assez longue. En cohérence avec d'autres observations du cycle annuel global, l'activité à méso-échelle augmente dès l'automne jusqu'au cœur de l'hiver, puis diminue régulièrement, au moins jusqu'à l'été. Les événements à méso-échelle paraissent avoir une extension verticale de quelques centaines de mètres, et la décomposition EOF a montré qu'il n'y avait quasiment pas de rotation des fluctuations avec la profondeur. Ces événements devraient avoir une structure verticale relativement simple, correspondant principalement au premier mode barocline dont l'ordonnée à l'origine est 400-500 m. Les courants sont relativement bien représentés par la combinaison du mode barotrope et du premier mode barocline, le barocline étant prédominant

et plus énergétique, en particulier en hiver. Par suite des variations du courant Nord, en largeur et en profondeur, le point le plus au large (30 km) se trouve soit en dehors, soit plus ou moins dans le courant, de sorte que le régime dynamique y est généralement complexe. Néanmoins, les événements à méso-échelle qui y sont observés sont, au cœur de l'hiver, les barotropes de la zone centrale, siège d'une convection vigoureuse. Les fluctuations ont généralement des échelles de temps intégré plus courtes en hiver qu'au printemps. À cause de transformations hivernales radicales, le courant Nord est instable et développe des méandres. Un résultat important révélé par les ellipses de dispersion et l'analyse spectrale est que ses principales fluctuations sont généralement quasi-transversales en son cœur même. De plus, d'après la polarisation de l'énergie, la signature de méandres cambrés de grande amplitude est nettement mise en évidence à 10-20 jours. Ces méandres ont beaucoup plus d'énergie en hiver qu'au printemps où leurs périodes sont légèrement plus courtes (10 jours). Comme déjà observé, des fluctuations à plus courtes périodes (3-6 jours) et de plus faibles amplitudes sont également associées à des méandres d'une autre nature; elles s'intensifient à partir de la période printemps-été jusqu'au cœur de l'hiver. Au printemps, tandis que le courant est plus stable, les fluctuations prédominantes sont assimilées à des pulsations du courant sur une largeur qui serait de quelques dizaines de kilomètres. Une observation fondamentale pour les problèmes d'océanographie côtière est le caractère aléatoire de la circulation dans une bande côtière d'une dizaine de kilomètres. Les principales caractéristiques saisonnières et à méso-échelle du courant Nord, en particulier les flux relativement élevés pendant la longue saison hivernale de formation d'eau dense, son rétrécissement et son rapprochement de la côte momentanés, ainsi que l'extension de la zone centrale au cœur de l'hiver, sont très probablement liés. Les auteurs retiennent comme hypothèse, pour les travaux expérimentaux et théoriques ultérieurs, que la formation hivernale d'eau dense pourrait être l'un des moteurs principaux forçant la circulation dans la partie nord de la Méditerranée occidentale.

INTRODUCTION

The general circulation in the western Mediterranean Sea is dominated by two major currents: the Algerian Current in the south and the Northern Current in the north. The consequence of the excess of evaporation over precipitation, throughout the Mediterranean Sea, is a mass deficit that is balanced by an incoming flux of Atlantic water through the Strait of Gibraltar. Downstream of the Alboran Sea, the Modified Atlantic Water forms the Algerian Current, which tends to flow eastward along the African coast. The unstable nature of this current leads to the formation of meanders and cyclonic and anticyclonic eddies that move eastward at a few kilometres per day, sometimes over a period of several months (Millot, 1987*a*); some of this author's hypotheses suggest that certain eddies are able to drift across the basin, interacting with the current, which is thus deflected seaward. Due to this instability, part of the surface water spreads into the interior of the Algerian Basin. Another part spreads through the Strait of Sardinia in the eastern Mediterranean and the Tyrrhenian seas. Flowing northeastward out of the Algerian Basin, a vein is identified as the Western Corsican Current. In the Ligurian Sea, it joins the Eastern Corsican Current coming from the Tyrrhenian Sea through the Corsican Channel, to form the Northern Current that flows southwestward throughout the year along the continental slope; this current is recognized as an entity as far as the Catalan Sea (Millot, 1987*a*; Font *et al.*, 1988; Lopez-Garcia *et al.*, 1994), with a flux of the same order (1-2 Sv) as the incoming and outgoing fluxes at the Strait of Gibraltar (Lacombe and Tchernia, 1972*a-b*; Béthoux *et al.*, 1982).

Crucial to the oceanography of the northern part of the western Mediterranean Sea is the central zone, dominated by dense water formation processes occurring in winter and surrounded to the north by the Northern Current. Different water masses can be recognized by their specific characteristics. Modified Atlantic Water (MAW), characterized by relatively low salinities, forms a surface layer to a depth of 200-300 m. Warmer and saltier Levantine Intermediate Water (LIW) spreads from the Sicily Channel at depths of 300-700 m, passing along the continental slope and leaving it on its right (Millot, 1987*a*). Due to the cyclonic circulation, the central zone is associated with a doming structure of the isopycnals, so that the stability there is relatively weak. The region is under the influence of intense exchanges with the atmosphere due to the strong, cold and dry northwesterly winds that blow in winter. These violent meteorological conditions constitute an efficient forcing to start intense cooling and evaporation which induce a density increase of the surface layer and initiate vertical mixing. In the current, this leads to the transformation of MAW into Winter Intermediate Water

(WIW), which is then recognized as a thin layer of relatively low temperature between MAW and LIW. Then, vigorous convection with vertical velocities of the order of some ten cm/s is induced by important instability processes and dominates the central zone (Gascard, 1978; Schott and Leaman, 1991). As a consequence of deep convection, Western Mediterranean Dense Water (WMDW) is formed in the central zone, where barotropic structures are characteristic, and spreads over the whole sea; it is found down to the bottom where it flows along the continental slope (Millot, 1994). One of the very few regions of the World Ocean where dense water formation occurs, which are essentially located in subpolar areas of both hemispheres (Norway, Greenland, Labrador and Weddell seas), the northwestern Mediterranean Sea has been the object of numerous studies devoted to the survey of these processes, mainly in the 1970s (MEDOC Group, 1970) and recently (Schott and Leaman, 1991). Relationships between the advective and convective phenomena have been put forward (Crépon and Boukthir, 1987); according to numerical models (Madec et al., 1991), the dense water formation could force, in deep winter, a cyclonic circulation that would persist throughout the year.

Other campaigns, carried out mainly in the Ligurian Sea, have furnished many observations which point to a seasonal variability of the circulation with a flux of the Northern Current that is higher in autumn-winter than in summer, but which are not in good agreement on the period of the flux increase. While hydrological data collected in the Ligurian Sea have suggested an increase of the flux of both the Eastern Corsican and Northern currents towards mid-autumn (Béthoux et al., 1982), current measurements in the Corsican Channel have shown an increase of the flux of the Eastern Corsican Current at the onset of winter (Astraldi et al., 1990). Recent hypotheses put forward by Astraldi and Gasparini (1992) can explain some specific features of this seasonal variability. The Eastern Corsican Current (0.8-1 Sv), which may be expected to be mainly driven by the different thermohaline conditions in the Liguro-Provençal Basin and the Tyrrhenian Sea, is maximum in winter. The Western Corsican Current (0.8-1 Sv), expected to be part of a large cyclonic gyre driven by the geostrophic adjustment to the winter dense water formation reaches its maximum several months later. Therefore, the Northern Current is expected to have a more complex seasonal variability and high flux values (1.6-2 Sv) induced by these maxima.

Another important feature of the Northern Current is its mesoscale variability which, from in situ and remote-sensing data as well as from analytical models (Crépon et al., 1982; Font, 1990; Millot, 1991; Sammari et al., 1995), mainly appears through meanders. These meanders can have a relatively wide range of wavelengths (a few 10 to 100 km), phase speeds of ~10 km/day and such amplitudes that they can affect the whole width of the current, i.e. a few tens of kilometres. Analysis of current measurements collected in the Ligurian Sea during the DYOME experiment (1981-1982) has also suggested that the mesoscale variability, which is especially intense in winter and is probably generated by instability processes of the current itself, spreads towards the open sea (Taupier-Letage and

Millot, 1986). The PROLIG-2 and PROS-6 experiments (May-December 1985), carried out in the same area, have also emphasized some aspects of the seasonal and mesoscale variabilities of the Northern Current, especially a predominance of the mesoscale phenomena in autumn in comparison with spring and summer (Sammari et al., 1995).

The PRIMO programme (Programme de Recherche International en Méditerranée Occidentale, 1989, 1991) was initiated to improve our understanding of the major forces which drive the circulation, its pricipal aim being to clarify the seasonal variability of the circulation, combining both experimental and theoretical studies. In order to investigate the seasonal and mesoscale variabilities of the Northern Current, the PRIMO-0 experiment was conducted in the Corsican Channel, the Ligurian Sea and the Channel of Ibiza, from December 1990 to May 1991, by several European teams. Some 60 current meters altogether were moored, about twice as many as in any previous experiment in the Mediterranean Sea. It is only through simultaneous observations of both the coastal zone, under the influence of the Northern Current, and the central zone, where dense water is formed, that evidence of likely relationships between the advective and convective phenomena may be expected; it was thus our intention to collect current measurements in both zones. In the Ligurian Sea, six moorings (out of nine, the three others being in the centre of the sea: Astraldi et al., this issue) supporting 30 AANDERAA current meters were set in place off Nice (Fig. 1). Among these, the best equipped were the mooring points (pts) 1, 2, 3 and 4, located respectively at ~8, 15, 20 and 30 km from the coast (schematized by a 240° T line passing by Cape Ferrat). The locations were chosen according to previous results (Taupier-Letage and Millot, 1986) with the aim of sampling both the coastal (pts 1, 2, 3) and central (pt 4) zones. A further element of our strategy was to observe mesoscale phenomena, especially meanders, as closely as possible. The signature of a sinusoidal meander, at fixed points, is recognized through transverse (with respect to the mean flow) fluctuations at its centre and parallel ones on its edges, the limit between both depending directly on the steepness. Moreover, the energy polarization must be anticlockwise on the outer edge and clockwise on the inner edge, while no direction must be preponderant in the middle of the meander, which corresponds to the core of the current. Nevertheless, mainly due to the variability of the width of the current, which proved greater than expected during this experiment, the chosen locations generally appeared to correspond rather to its inner (pt 1) and outer (pt 4) edges, the core being located at 15-25 km (pts 2-3). A fortnightly hydrological survey, from October 1990 to July 1991, at 13 equally-spaced (~4 km) stations situated between ~6 and 55 km from the coast (Fig. 1), complemented these current measurements; nearly 250 CTD casts were collected in the course of some twenty surveys. The PROLIG-2 and PROS-6 observations, collected between May and December 1985, have shown some similar characteristics with the DYOME observations obtained further seaward over a

Figure 1

Locations of mooring points and CTD stations during PRIMO-0. The bathymetric contours are in metres.

PRIMO - 0
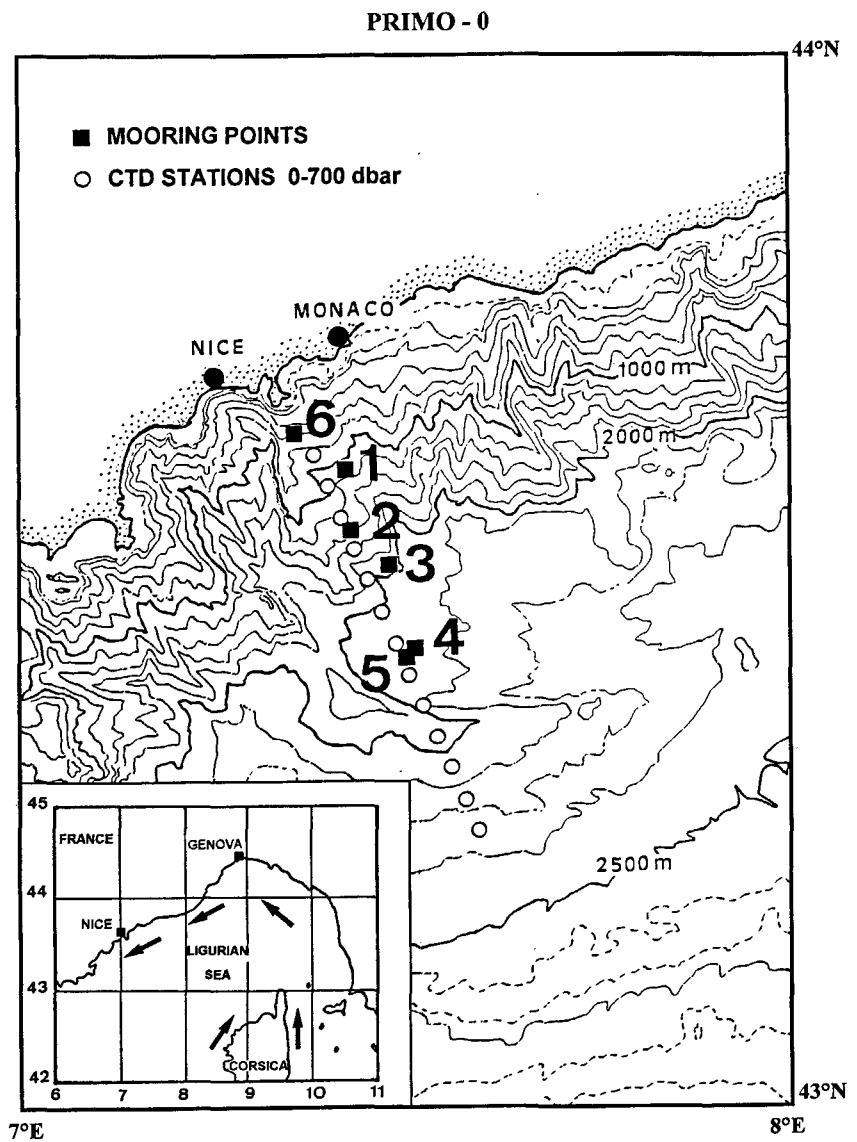
full year (1981-1982). Our own observations, collected from December 1990 to May 1991 in the same area as PROLIG-2 and PROS-6, also indicated such similarities. Therefore, despite the interannual variability, we advance as justified the hypothesis that the addition of the PRIMO-0 experiment to the PROLIG-2 and PROS-6 experiments may be expected to provide enlightenment concerning the characteristics of the Northern Current throughout a complete annual cycle.

The purpose of this paper is to present a description and a synthesis of the seasonal and mesoscale variabilities of the Northern Current, from the PRIMO-0 data sets collected off Nice. The hydrological data and current measurements are described in section 2. The fluctuations of the current are first analysed from the basic statistics of the time series (section 3). We proceed in section 4 with the empirical orthogonal decompositions of the velocity field, complemented with the determination of the dynamic vertical modes. Investigation of the frequency spectra permits clarification of the scale and nature of the fluctuations (section 5). Finally, the results are synthesized and discussed in section 6.

DESCRIPTION OF HYDROLOGICAL AND CURRENT MEASUREMENTS

Hydrological data

The temporal and spatial sampling is relatively fine but still rather rough considering the mesoscale variability emphasized by the current measurements (see § Current measurements). It has produced better evidence of the mesoscale variability but does not permit its resolution; it is consequently difficult to differentiate with certainty the mesoscale and seasonal variabilities.

Hydrological characteristics

The fortnightly hydrological surveys (generally down to 700 dbar) provide us with information on the characteristics (potential temperature θ, salinity S and potential density σ_θ) and distribution of MAW, WIW and LIW. Due to the large number of sections of these parameters, only representative ones are presented in Figure 2; otherwise, some isolines are specified. The major seasonal variations,

concerning mainly the spreading of LIW in an on-offshore direction, the formation of WIW and the advection of less modified MAW, can be depicted as follows.

In October (Fig. 2a), MAW is relatively warm and fresh (θ = 13-20 °C, S = 37.8-38.3) and the width of the current is more than 40 km; the isopycnals (σ_θ = 27.0-28.9) have a very smooth slope. The core of LIW, well defined by its relative maxima ($\theta \sim 13.54$ °C, S~38.56), is located relatively close to the coast at 20-25 km and at depths of 400-500 m. The vein of LIW spreads along the isopynals, the slope of which is a little steeper than above (the 29.05 isopycnal is found at ~500 and 300 m at ~5 and 55 km, respectively).

Up to late November, similar characteristics are observed, with a progressive cooling of the upper MAW layer ($\theta < 15$ °C) which starts to become denser ($\sigma_\theta > 28$). The core of LIW ($\theta \sim 13.58$ °C, S~38.56) has clearly spread seaward, rising along the ~29.05 isopycnal, and is then found as far as ~40 km from the coast, mainly at 300-400 m, the depth increasing with distance.

In December, sustained by the winter meteorological conditions, the cooling continues and overtakes the whole MAW layer. The core of LIW appears to have returned shoreward, since it spreads within a coastal band of ~20 km, indicating clear seasonal variations of its location in the on-offshore direction. From late January to mid-
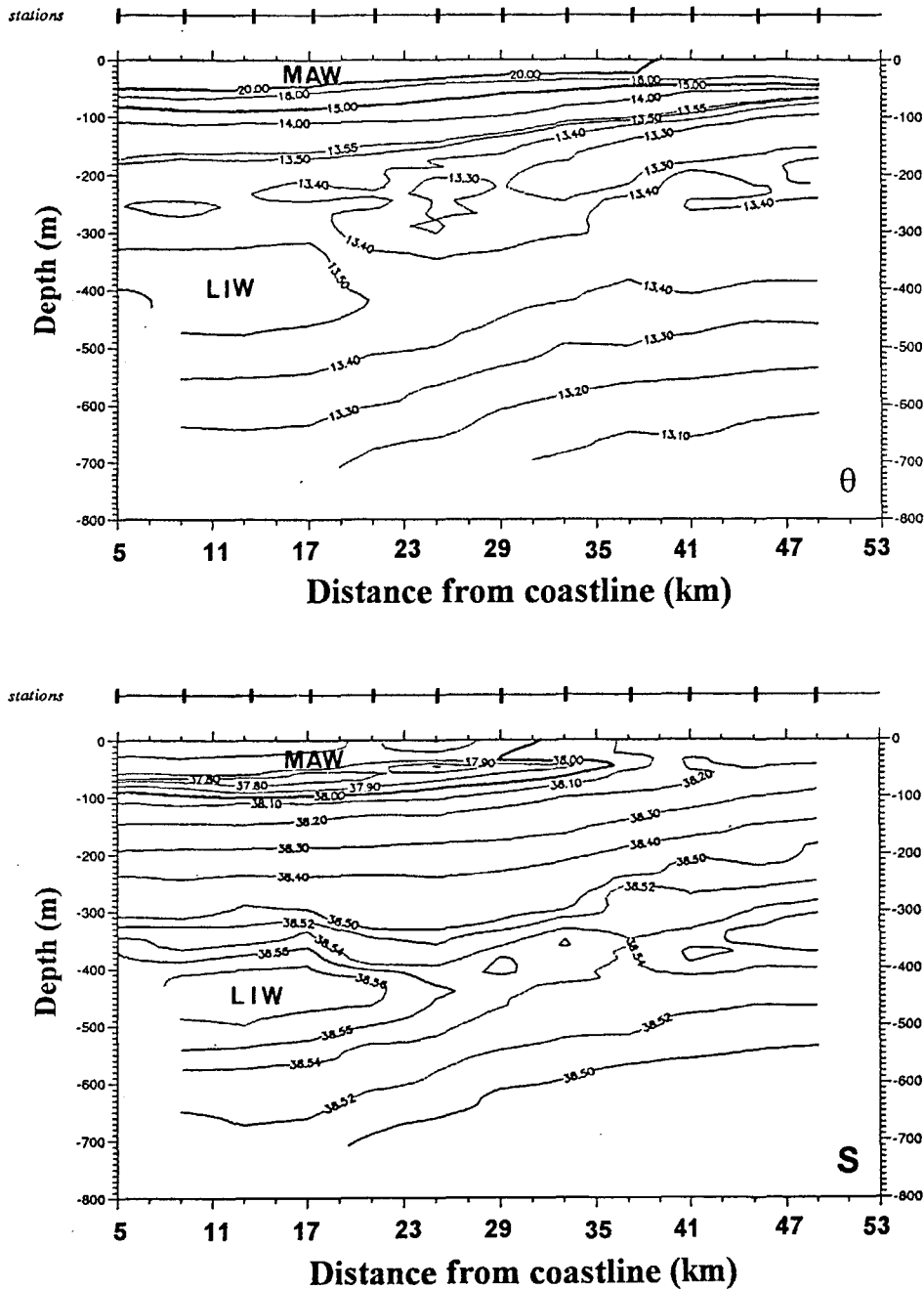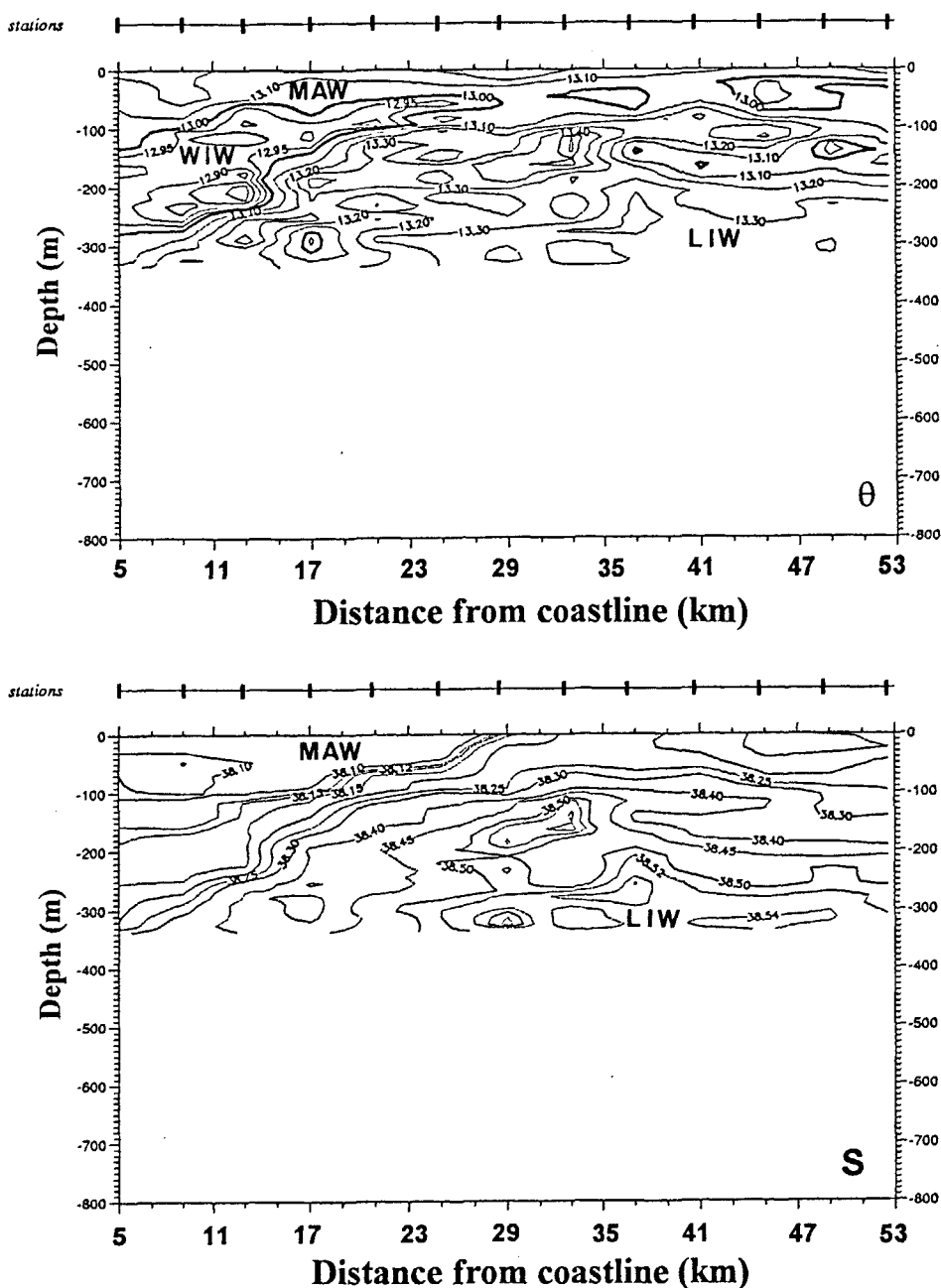

Figure 2a

Figure 2b

March, we were unfortunately constrained on four occasions to use a CTD which could go no deeper than 300 dbar, so that LIW could not be completely surveyed. Nevertheless, some features have been noticed in the upper layer.

In late January, the isolines are very steep and vertical mixing, occurring along the isopycnals, leads to a relatively cool and homogenized MAW (θ < 13.56 °C, S = 38.05-38.20 and σ_θ > 28.64).

In late February, MAW has been so strongly cooled and mixed that it is now well homogenized and denser than before (θ = 13.0-12.9 °C, S = 38.12-38.20 and σ_θ > 28.82). A relatively thin layer of WIW has been formed, clearly distinguishable with θ minima as low as 12.72-12.77 °C; the core of WIW is found at 30-35 km between 100-200 m. The MAW overlying WIW is thus less modified

MAW which has been advected. The isopycnals rise at 25-30 km and display a doming structure, the top of which is located at ~40 km; this results in a relatively dense (σ_θ = 28.85-28.88) and homogenized surface layer.

In early March, the situation is similar, but now a part of LIW (θ~13.51 °C, S~38.56) appears from ~30 to 50 km at depths of 200-300 m, as if having spread seaward following the dome of the isopycnals, while the formation of WMDW begins.

In mid-March (Fig. 2b), a noticeable feature is that WIW is found closer to the coast at depths of ~200 m and shallower when progressing seaward to a distance of ~25 km.

At the end of March, MAW starts to become warmer (θ = 13.1-13.7 °C) and the surface densities are lower (σ_θ = 28.55-28.75) than previously (σ_θ = 28.75-28.80), accounting for advection of less modified MAW. Due to
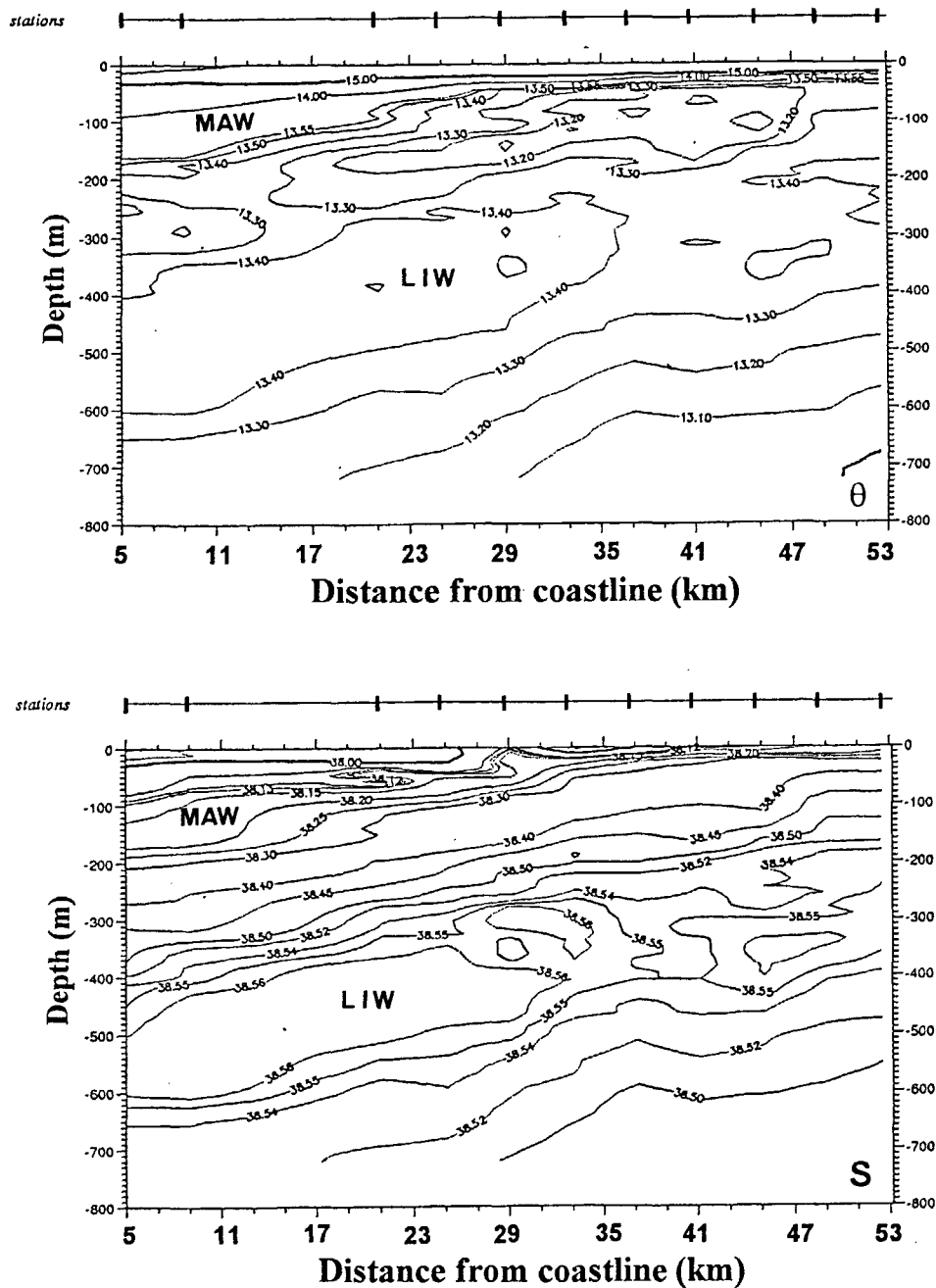
Figure 2c

Potential temperature (°C) and salinity on 18 October (a), 11 March (b) and 12 June (c).

vertical mixing, LIW has been homogenized so that its temperature (θ~13.30 °C) is generally lower than before over the major part of the vein, while the formation of WMDW continues; its core, characterized by θ~13.53 °C and S~38.55, is relatively small and located at less than 25 km.

In April, the MAW layer warms up to ~14 °C. LIW has spread seaward along the isopycnals 29.05-29.07, as far as ~40 km, and its wide core (θ~13.54 °C, S~38.56) lies within 20-30 km between 200-400 m; in mid-April, the values in the core have increased up to θ~13.58 °C and S~38.58.

In May, stratification starts in the upper MAW layer, with θ as large as ~16 °C, S = 38.0-38.1 and σ_θ = 28.0-28.5. The vein of LIW, mainly characterized by a temperature (θ~13.40° C) lower than usual, spreads seaward along the

isopycnals further than before, almost over the whole section; its core (σ_θ = 13.50-13.52 °C, S~38.56) is found as far as ~50 km in a very thin layer at ~200 m.

In June (Fig. 2c), similar features are observed while the stratification progresses; LIW (θ = 13.40-13.47 °C, S = 38.55-38.56) lies from ~5 to 55 km, the maxima being observed near the coast at less than 20 km.

In July, the stratification is well established and the mixed layer is warm (θ~20 °C) with low salinities (S = 37.8-38.2) and densities as low as σ_θ ~26. The isopycnals are again very smooth and the LIW vein (θ = 13.40-13.54 °C, S = 38.55-38.56) continues to spread seaward along them (σ_θ = 29.05-29.06), lying throughout the section at 400-500 m, and to such a distance that the outer boundary of the vein has not been sampled.

170

These observations throw into relief the importance of the mesoscale phenomena which modify both the MAW and LIW layers. As regards the formation of WIW, it seems that MAW is first cool and homogenized by the strong, cold and dry winds and then rapidly overlaid by less modified MAW

which is advected when the winds cease. From that point, the part of MAW that is cool and overlaid by less modified MAW will be recognized as WIW, by its specific minimum in temperature. On the whole, LIW shows some seasonal variations of its hydrological parameters and its distribution. Generally, it forms a vein along the continental slope with the core at 20-30 km, but the mesoscale phenomena can move the core noticeably seaward, especially in winter. LIW seems to be able to spread seaward, at the beginning of the formation of WMDW; it is then characterized by relatively low temperature and salinity maxima, due to intense vertical mixing. From spring, although the vein of LIW still extends over a few tens of kilometres, its core is again usually close to the coast (20-30 km) and the highest in temperature and salinity maxima are observed (θ~13.58 °C, S~38.58).

Geostrophic currents

The geostrophic currents have been computed with a reference level at 700 dbar, except on four occasions between late January and mid-March when we used the 300-dbar CTD. The reference level at 700 dbar is convenient, considering the very low measured currents (see the stick-diagrams in Fig. 6). The measured currents at 300 dbar are generally of the order of 2-3 cm/s, thus the difference with the 0 cm/s imposed by the reference level is relatively weak, and the results are significative. Note that this choice does not alter the structures that can be compared.

The seasonal variability of the Northern Current is rather well depicted by some vertical sections of the geostrophic current (Fig. 3).

In October (Fig. 3a), the quasi horizontal isotachs display a wide and shallow current; the 10 cm/s isotach, found between 100-200 m, intersects the surface at ~10 and 50 km and the core of the current (50-60 cm/s) is located at ~30 km from the coast. Such a wide and shallow current is frequently observed at least until November-December. Figure 3b is representative of the structure of the current observed from at least late January to mid-March, showing very steep or even quasi vertical isotachs, the signature of a narrowing and deepening of the current which flows closer to the coast. The 10 cm/s isotach is at the surface at ~10 and 30 km and the core is at less than 20 km. During this deep-winter season, the maximum speeds are lower than in autumn, ranging within 20-40 cm/s; note an opposite flux beyond the outer edge of the current, with maximum values of 10 cm/s.

From the end of March, the current displays more complex structures which might correspond to intermediate stages, before recovering from May to July (Fig. 3c) a wide and shallow structure that it will more or less maintain till autumn (Sammari et al., 1995). Hence, the Northern Current is most of the time wide (~40 km) and shallow, except from late January to mid-March when it appears narrower (~20 km) and deeper, flowing closer to the coast.
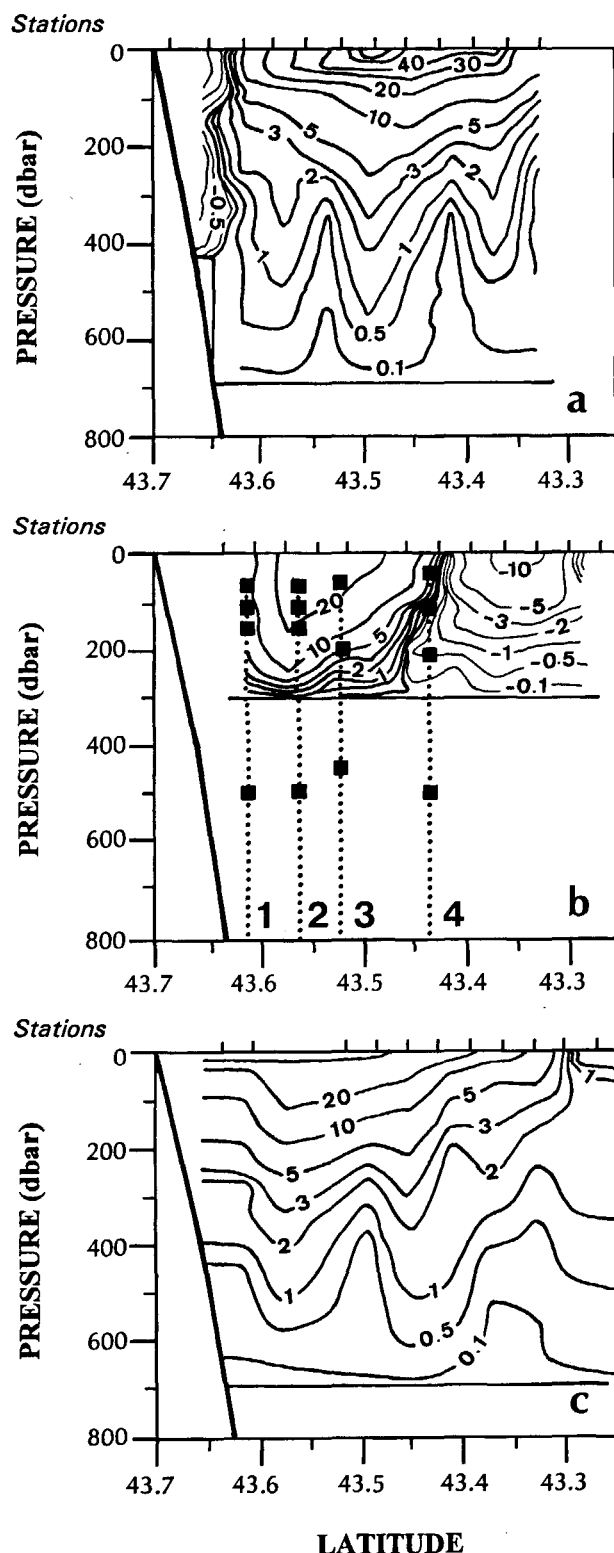

Figure 3

Geostrophic current (cm/s) on 18 October (a), 11 March (b) and 12 June (c). The reference level is either 300 or 700 dbar, according to the CTD used. Locations of the mooring points with the current meters are indicated in (b).

From the vertically integrated flux computed between pairs of stations, in October (Fig. 4a) the flux is maximum at ~30 km and the outer edge is reached as far as ~50 km,

indicating a relatively wide (~40 km) current, as described above (Fig. 3a).

At the end of October, a different structure has been evidenced with the maximum flux at ~50 km, *i.e.* where the outer edge was previously observed, separated from the coast by an opposite flow ~15 km in width. The corresponding vertical section of the geostrophic current (not shown) displays maximum speeds of ~40 cm/s within the core of the current and ~15 cm/s in the opposite flow.

In November-December (Fig. 4b), the core of the current, usually within 20-40 km, can be found very close to the coast at ~10 km. On the vertical sections of the

geostrophic current (not shown), the 10 and 30 cm/s isotachs can intersect the surface offshore at ~40 and 15 km respectively and slope very steeply shoreward to reach ~350 and 150 m below the core when it is very close to the coast (~10 km), thus accounting for a strong shear of the current.

From late January to mid-March (Fig. 4c), despite the intense mesoscale variability, the maximum flux is generally observed closer and closer to the coast which might account, on the whole, for some seasonal variations. During this season, the flux values are highest in March, when the current is narrowest (~20 km).
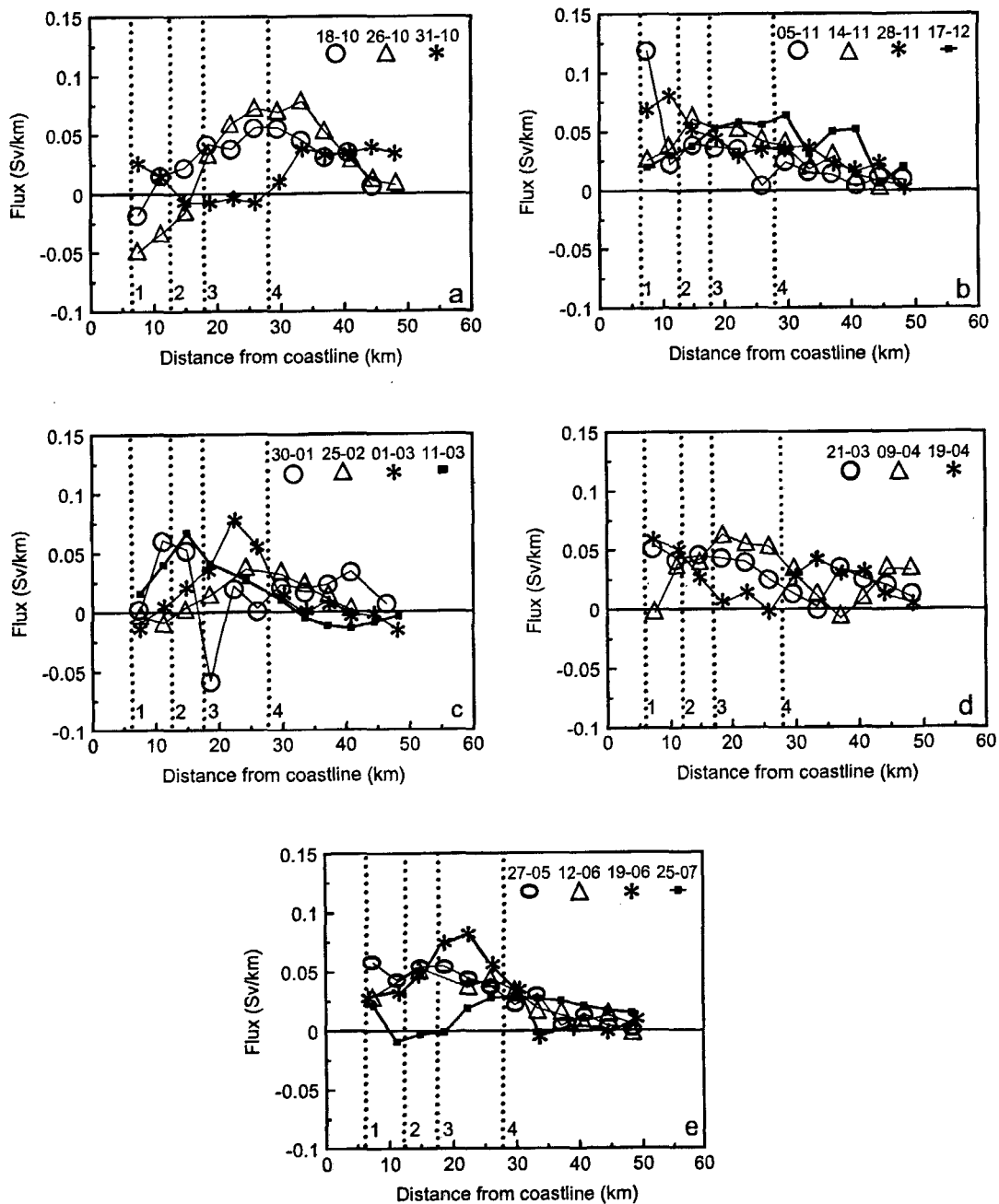

Figure 4

Vertically integrated flux computed between pairs of stations from autumn 1990 to summer 1991 (a to e). For visibility, we have sorted 3 or 4 curves in a same figure, more or less according to their shapes. The reference level is 700 dbar, except in (c) where it is 300 dbar. The locations of the mooring points are indicated by dotted lines.

From the end of March (Fig. 4d), the vertically integrated flux does not emphasize any clear evolution of the structure of the current which is more complex and varying during some intermediate stages, as supposed above.

From May to July (Fig. 4e), the current tends to become again wide and shallow.

In brief, from the vertical sections of the geostrophic current and the vertically integrated flux, the Northern Current appears to be usually relatively wide and shallow, with a well-defined episode of narrowing, deepening and shoreward shift from late January to mid-March.

The variability and the complexity of the structure of the Northern Current, on both the horizontal and the vertical planes, underscore the difficulty of obtaining an accurate estimation of the flux. If the discrepancies between the values reported in the past, whether via hydrological data (Béthoux et al., 1982) or through current measurements (Astraldi et al., 1990), can appear relatively large, they are not inconsistent but just not immediately comparable. Moreover, the use of different kinds of data with non-convenient hypotheses can lead to reversed conclusions with regard to the maximum flux, according to the structu-

re of the current; indeed, the major part of the flux, sometimes concentrated within a few tens of metres of the superficial layer of a wide and shallow current (as in Fig. 3a), can be missed by insufficiently shallow current measurements (Albérola, 1994).

Since the hydrological casts were close to the moorings, we can compare the fluxes estimated from each kind of data. However, there is no single definition of the Northern Current and of its flux, and because of the intense seasonal and mesoscale variabilities it is not easy to determine how it may be computed. So, to have an idea of the influence of the different possible definitions, we have computed the geostrophic flux in three different ways. First, the geostrophic flux limited to the mooring area (Fig. 5a), between 60 and 150 m, has been compared with the flux component perpendicular to the section obtained from the current measurements, using the mean current over the same depths, i.e. over a layer where similar currents are emphasized by the stick-diagrams (see § Some main features and Fig. 6). Note that the agreement between both estimations is very good, the largest differences being due to the mesoscale variability. Second, the Northern Current has been arbitrarily defi-
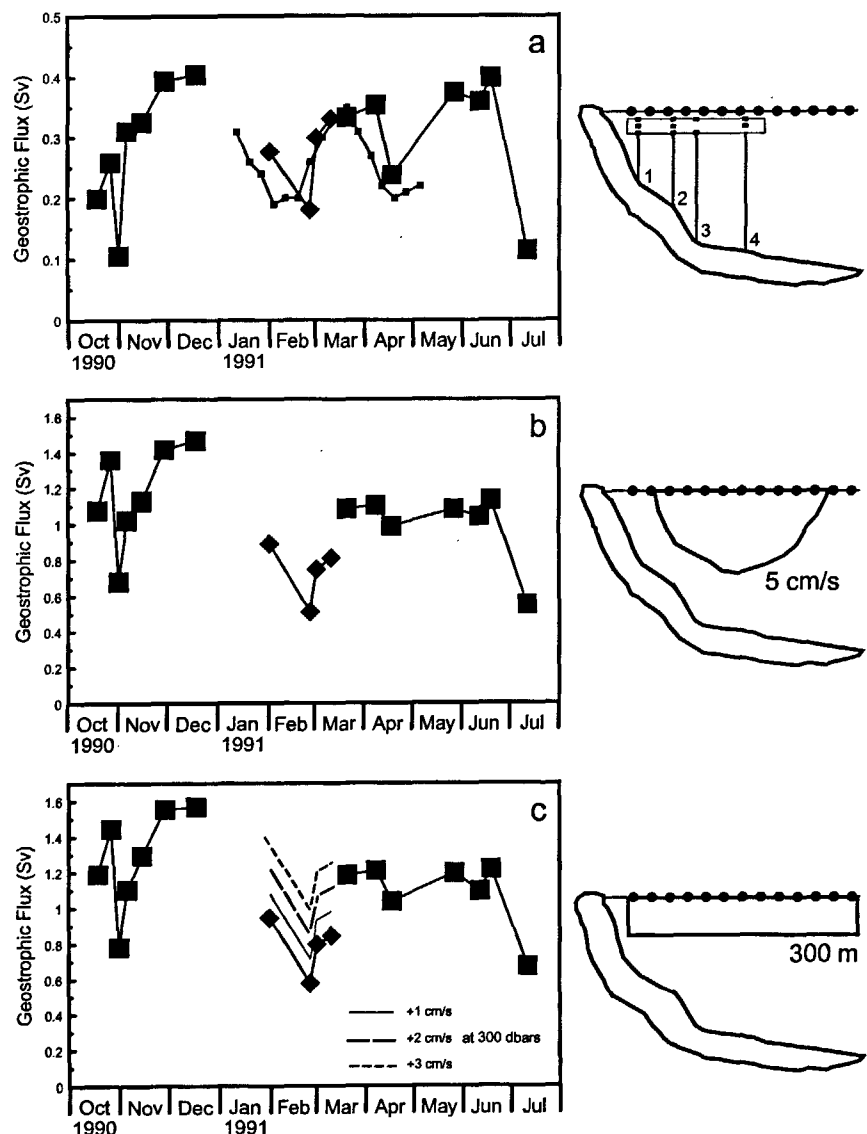

Figure 5

Temporal evolution of the geostrophic flux computed in three different ways: (a) limited to the mooring area between 60 and 150 m to compare with the flux computed from the current measurements (—■—), (b) through the area delimited by the 5 cm/s isotach, (c) through the whole hydrological section down to 300 dbar. The reference level is either 300 dbar (♦) or 700 dbar (■). The CTD stations are indicated by ●.

ned by the 5 cm/s isotach and the corresponding flux is represented in Figure 5b. The values obtained are in agreement with the known ones. Finally, the geostrophic flux has been computed over the entire hydrological section (Fig. 5c), integrated down to 300 dbar, which is the deepest common level. According to the current values generally measured at ~300 dbar (see Fig. 6), a speed of 1, 2 and 3 cm/s has been assumed at the shallowest reference level. Thus, the flux referred to 300 dbar increases by ~0.1, 0.3 and 0.4 Sv, respectively; with a correction of 2-3 cm/s, this flux is consistent with the one referred to 700 dbar. The three representations of the variations with time of the geo-

strophic flux have a similar shape. Figures 5b and 5c display values ranging most of the time between 1 and 1.6 Sv which are in good agreement with previous ones reported by Béthoux et al. (1988) and Sammari et al. (1995). Values that are sometimes noticeably out of this range are in all likelihood due to the mesoscale variability. Although this variability is clearly important, the temporal flux evolution tends to emphasize a rather long winter season characterized by relatively high values. Indeed, the flux is maximum in December with ~1.6 Sv and then, tends slowly to decrease until at least July (~1 Sv). Therefore, the maximum in December probably corresponds to that reported by
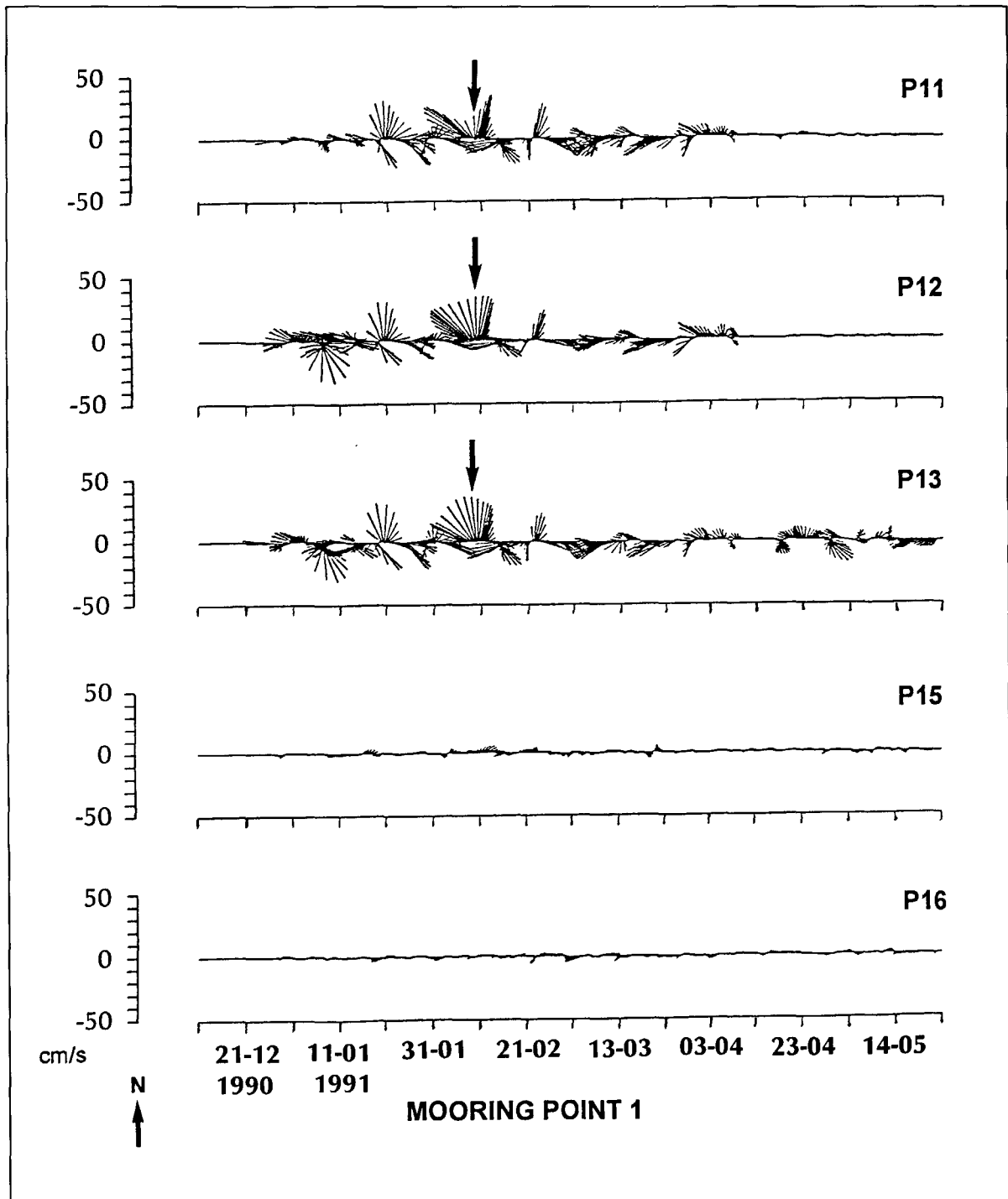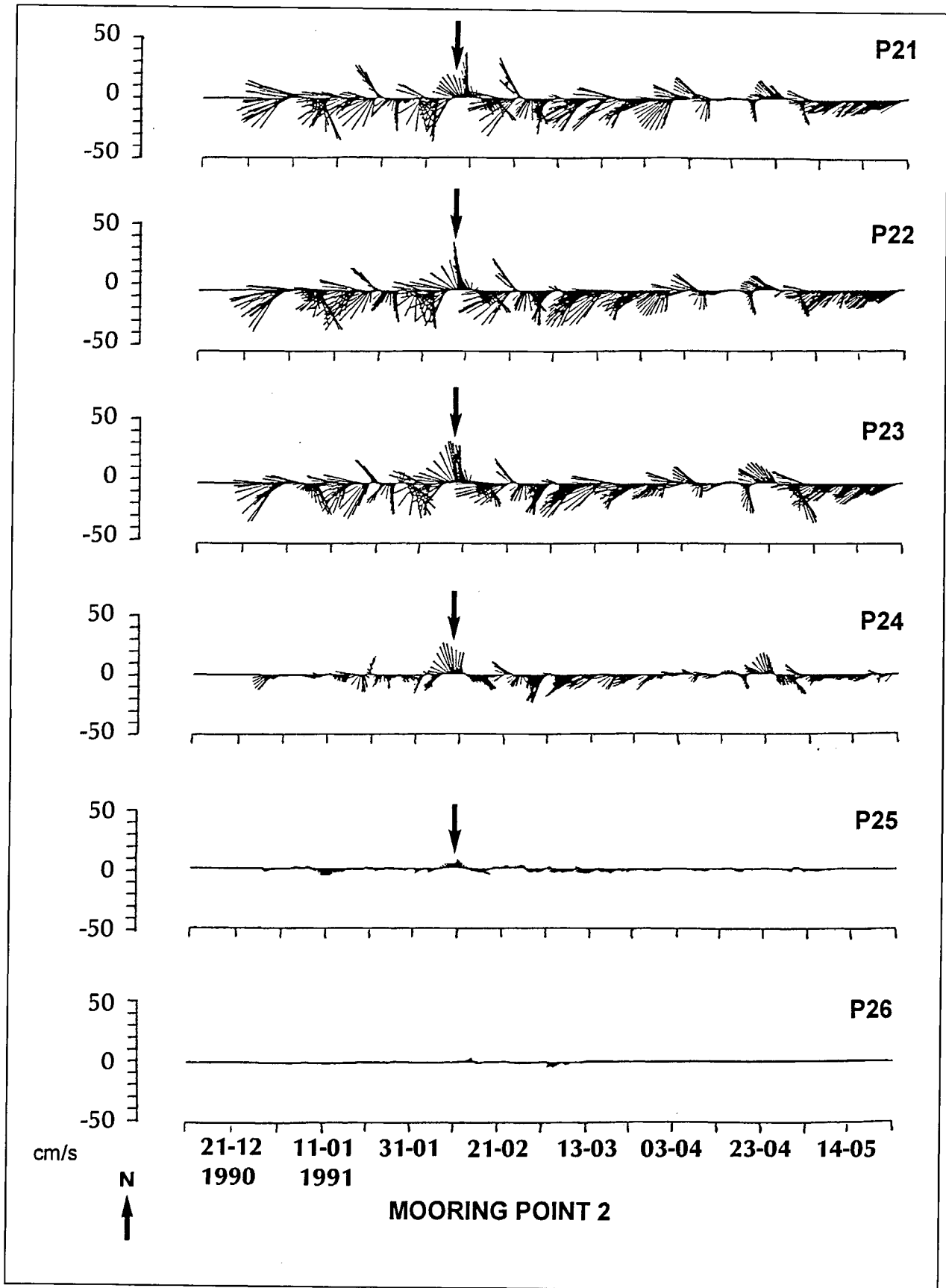

Figure 6a

174

Figure 6b

Béthoux *et al.* (1982) and, as hypothesized by Astraldi and Gasparini (1992), might be due to the maximum of the Eastern Corsican Current, while the still-large values observed in winter might be due to the maximum of the Western Corsican Current. The decrease from spring is coherent with the characteristics described by Sammari *et al.* (1995) who
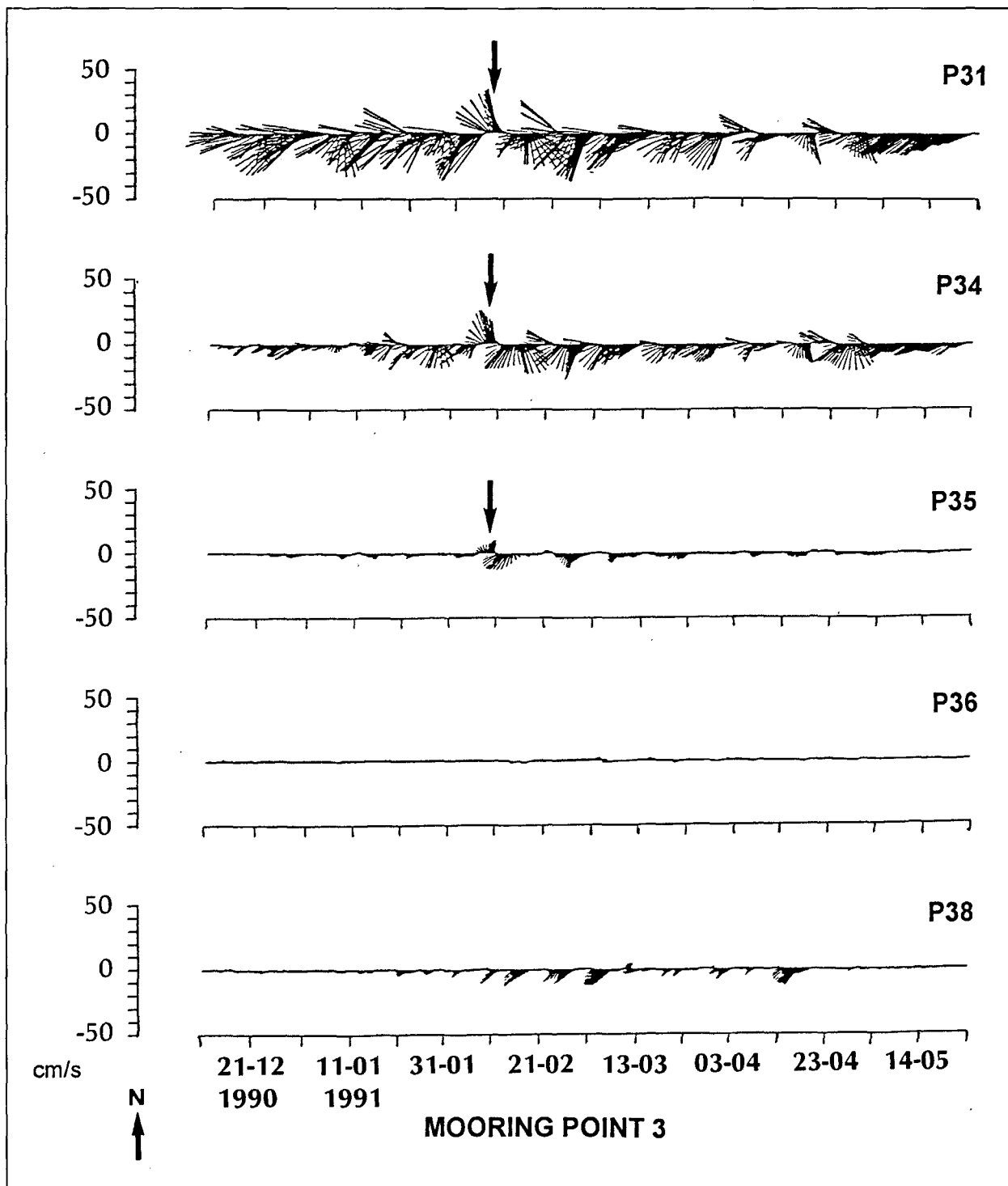
Figure 6c

account for no marked variations from spring to early autumn. Our own results thus lead us to agree with theirs, accounting for a consistent whole over a complete annual cycle.

Current measurements

Six (at pts 1, 2) to eight (at pts 3, 4) current meters were immersed at nominal depths of 20-60, 100, 150, 250, 500, 1000, 1500 and 2000 m. Each time series will be denoted by "P" and two numbers signifying respectively the mooring

point and the level (for instance, P44 indicates the time series at pt 4 at 250 m). The nominal depths were chosen as being identical for each mooring and despite slight actual differences (by 10-40 m at pts 3 and 4), we will assume them to be equal. Technical problems at pts 3 and 4 made some current time series unavailable (P32, P43), as are others (P14, P33, P37) due to instrumental failures. Here we deal only with the time series collected at pts 1 to 4; moorings 5 and 6 supported only one current meter with respectively an ADCP (Acoustic Doppler Current Profiler) and a tide gauge, and will be analysed elsewhere. The length of the records is generally 146 days (from 27 December 1990
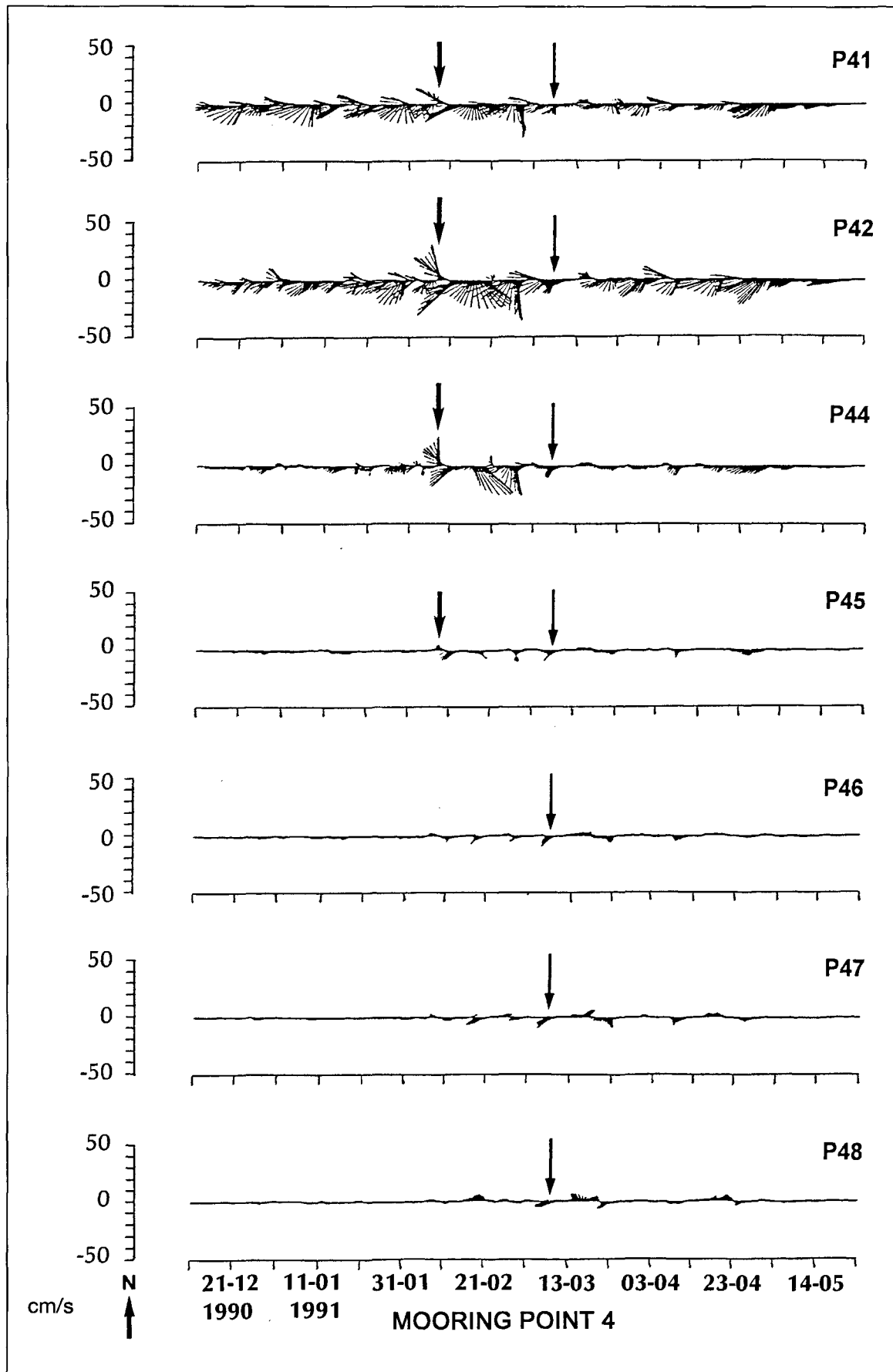
Figure 6d

Six-hourly stick-diagrams of the current at pts 1 (a), 2 (b), 3 (c) and 4 (d), at each depth. The hourly current components are low-pass filtered through 40 h and subsampled at 6-hour intervals. As an example, a mesoscale event recognized at each point at various depths is indicated by heavy arrows and a barotropic event specific to pt 4 is indicated by thin arrows in (d).

to 23 May 1991), except P11 and P12 which last 102 days and P26 only 79 days. The current measurements, sampled at hourly intervals, have been low-passed through a Lanczos filter (Roberts and Roberts, 1978) using a cut-off period of 40 h, and subsampled at 6 hour intervals. These 6-hourly time series have been used for most of the statistical ana-lyses, unless otherwise specified.

Some main features

The stick-diagrams of the current time series have been plotted in Figure 6. At pt 1 (Fig. 6a), it first appears that the currents are very similar, at least between 60 and 150 m (three upper levels). In this layer, it seems that quasi no mean current is observed, whereas the mesoscale events are predominant and especially intense in January-February (see, for instance, the sticks from early to mid-February). The currents at the deeper levels are rather different from those above and relatively low. At pt 2 (Fig. 6b), the cur-rents at the upper levels are similar, also between at least 60 and 150 m. The mean southwestward direction of the circulation clearly appears at these levels, despite the fact that mesoscale events are still especially intense in January-February as at pt 1. Some of these events can be recognized over some few hundreds of metres (see, for instance, the sticks in mid-February), but the currents at the deepest level are rather low. The stick-diagrams at pt 3 (Fig. 6c) emphasize similar current directions at the two upper levels (50 and 200 m) with a slightly smaller amplitude at the second one, thus one can expect similar currents at least over the same upper layer as at the other points. The fre-quent southwestward direction of the sticks indicates that the mean current is important at these upper levels, although the signature of the mesoscale variability is noti-ceable, again often in January-February. This variability appears through events that can be recognized roughly over the same depth interval as at pt 2 (see also the sticks in mid-February). Note that the current values at the foot of the continental slope are relatively large; the mean and 6-hour maximum values are ~3 and 18 cm/s at P38, while they are only ~1 and 7 cm/s at P36. At pt 4 (Fig. 6d), the currents at the upper levels are similar over nearly the same depth interval as noted at the other points. The mean cur-rent can still be observed at these levels but appears to be less intense, probably due to the offshore location of this point. The mesoscale events are still predominant in Janu-ary-February, but have generally smaller amplitudes than at the previous points. Nevertheless, if these events are also usually recognized at several depths (for instance, in mid-February), an observation specific to this point is that they become deeper and deeper from February, until they obtain a barotropic structure towards mid-March over the whole 2000 m depth, characteristic of the central zone.

In view of all the stick-diagrams, pts 2 and 3 are within the Northern Current and often in its core, whereas pts 1 and 4 have more complex positions, described in the following, since they can be alternatively within or outside the cur-rent. However, the especially fine vertical resolution clear-ly emphasizes, at least from December to May, a layer bet-ween ~60 and 150 m where currents are similar,

irrespective of the location of the point (inside or outside of the current). This layer, which we will term the upper layer, is topped by the few tens of metres of the superficial layer evidenced from hydrological data, where the flux is concentrated when the current is wide and shallow (§ Hydrological data). The currents are expected to be similar from the upper layer up to the surface. The meso-scale variability, especially intense in winter, appears through events that can be recognized often over the entire width of the current (or at least over the ~20 km between pts 1 and 4). These events have relatively large ampli-tudes, of the same order as, or sometimes larger at the coastal point (pt 1) than at the others. They can reach various depths, usually ~500 m, but sometimes ~1000 m and even down to the bottom (~2000 m) at pt 4, in specific situations when the barotropic structure of the central zone is observed. The particular feature at the foot of the conti-nental slope (P38) has been already evidenced in the same area (Sammari *et al.*, 1995), as well as in other parts of the sea (Millot, 1994), so that it probably accounts for an iden-tical phenomenon which could be induced by interactions between the current and the topography.

Seasonal variability

Since the upper current meters at each point appear to be more or less in a single upper layer of ~100 m thickness, we have thought it efficient to analyse the seasonal varia-bility of the Northern Current through its monthly mean component parallel to the coast, computed over this upper layer at each mooring point (Fig. 7).

In January, the values at pts 2, 3 and 4 are large with mean speeds of 15-30 cm/s, so that these points appear to be inside the current, while the low values at pt 1 account for its location outside the current.
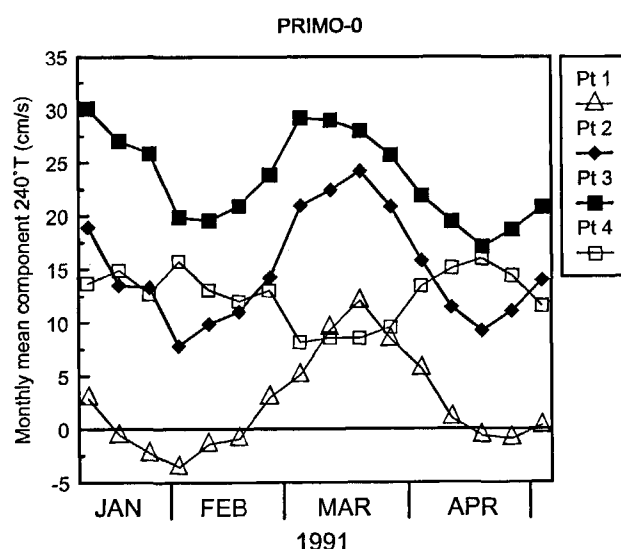

Figure 7

Monthly mean component of the current parallel to the coast (240°T) in the upper layer (i.e mean of the 60, 100, and 150-m levels at pts 1 and 2, 50-m level at pt 3 and 20 and 110-m levels at pt 4). Values are one-week spaced.

From late January to February, similar values are observed but, as evidenced by the geostrophic vertical sections, this is a period when the current becomes narrower and deeper, and tends to flow closer to the coast, and when the mesoscale events are especially intense as shown by the stick-diagrams (Fig. 6).

From late February, the mean flow thus starts to be perceptible at pt 1, while it slowly decreases at pt 4. These transformations of the structure of the current continue until mid-March: then, pt 1 is inside the current (mean speeds of ~10 cm/s), whereas pt 4 is rather on its outer edge, supporting a current that is especially narrow (~20 km) and very close to the coast (inner edge at less than 8 km).

From April, the mean flow decreases at pt 1, now mainly on the inner edge, while it increases at pt 4, and the trend is again towards a wide and shallow current with similar values at pts 2, 3 and 4, although these values are lower than in January.

Therefore, due to the complexity and variability of the structure of the current, the observations at pts 1 and 4 are at time quite different. Point 1 can be either quite outside the current (as often in winter), or on its inner edge (as often in spring), or even inside the current during a brief period (twenty days towards mid-March) when the current has moved shoreward. Conversely, pt 4, which is most of the time inside the current or sometimes rather on its outer edge (as often in the deep winter), can show the characteristic features of the central zone, as the barotropic structure observed towards mid-March (Fig. 6d) when the current flows closer to the coast.

In brief, the analysis of the seasonal variability of the Northern Current, through its monthly mean alongshore component, emphasizes its varying structure: its width is usually larger than ~30 km and the core is at more than 20 km, except in the deep winter when its width can be lower than 20 km, the core being closer to the coast. This seasonal evolution of the structure of the current is in good agreement with that deduced from the hydrological data, so that both kinds of observations are consistent and complement each other in depicting the Northern Current as being generally wide and shallow, except from late January to mid-March when it shows a narrowing, deepening and shoreward shift.

Mesoscale variability

The variance of the current in the upper layer (using the mean components over this layer) has been defined by $(\sigma_u^2 + \sigma_v^2)/2$ over one month (Fig. 8), as an estimate of the mesoscale activity following Taupier-Letage and Millot (1986).

In January, when the Northern Current has been depicted as remaining relatively wide and shallow, the mesoscale activity increases very fast at each point.

In February, the highest values are reached, accounting for an especially intense mesoscale activity in the deep winter, as expected from the large mesoscale events displayed on

the stick-diagrams (Fig. 6), while the current becomes narrow and deep.

From late February to mid-March, when the current is especially narrow, deep and close to the coast, as described from Figure 7, the mesoscale activity decreases markedly at all points.

From mid-March, while the trend is to a wide and shallow current, the mesoscale activity has relatively small values that will be maintained until early autumn (Sammari *et al.*, 1995). A similar trend to open sea propagation (Taupier-Letage and Millot, 1986) appears here again since the mesoscale activity seems to spread seaward, fading away to display smaller peaks but still shifted in time in the centre of the Ligurian Sea, evidenced from the simultaneously collected current measurements (Astraldi and Gasparini, personal communication). Therefore, it is clear that this mesoscale activity propagates towards the open sea, whatever its origin.

The progressive vector diagrams (PVD) indicate some clear differences a few kilometres apart, especially between pts 1 and 2, and demonstrate the intense mesoscale variability in space and time. Considering, for instance, the stick-diagrams at P13 and P23 (Fig. 6a, b) separated by ~7 km, a high mesoscale coherence can be noted. However, the relative importance of the mean circulation is more clearly shown by the PVDs (Fig. 9): pt 2 is always inside the current, whereas pt 1 is inside during only a brief period. Therefore, an essential feature is that for the greater part of the time, there is no significant mean current in a coastal zone of some kilometres, in other words the so-called general circulation is not observed there. These observations are of fundamental importance for coastal oceanography, which has to deal with such an unforeseeable circulation.
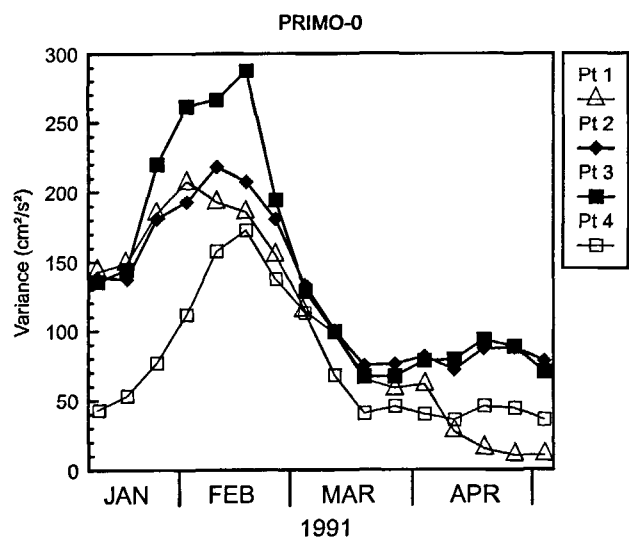

Figure 8

Variance of the current in the upper layer (i.e using mean components of the 60, 100, and 150-m levels at pts 1 and 2, 50-m level at pt 3 and 20 and 110-m levels at pt 4), defined by $(\sigma_u^2 + \sigma_v^2)/2$ as an estimate of the mesoscale activity, computed over one month. Values are one-week spaced.
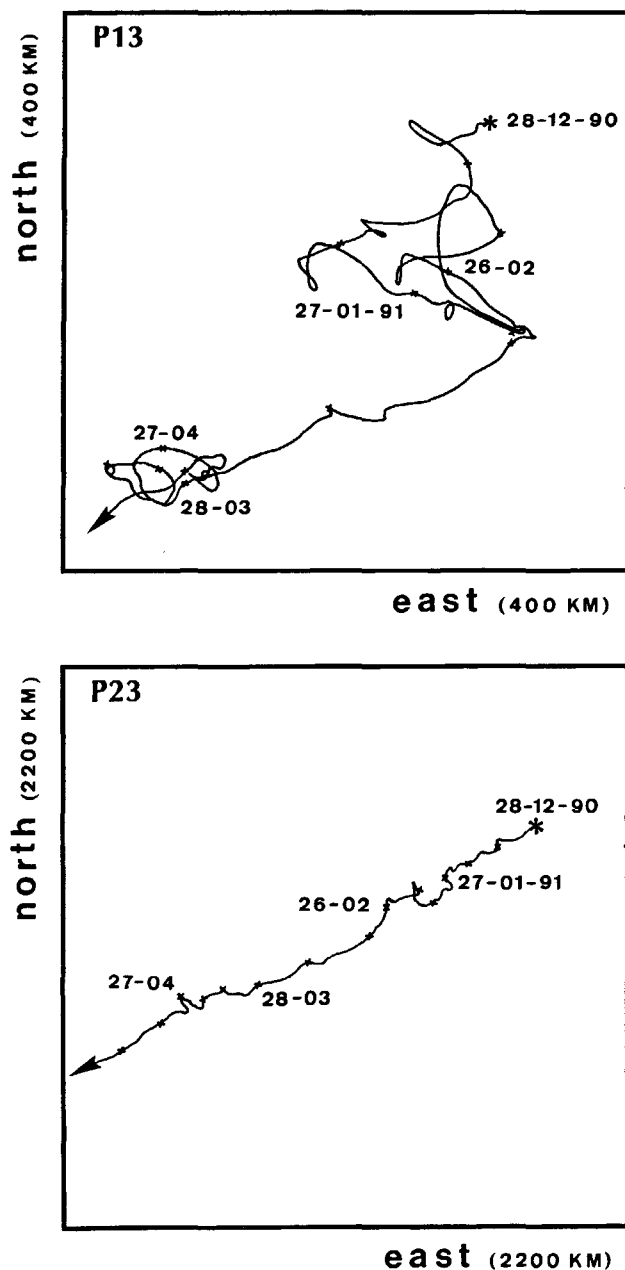
Figure 9

Progressive vector diagrams at pts 1 (P13) and 2 (P23), ~7 km apart.

Temperature records (not shown) display relatively large fluctuations, sometimes as large as ~1 °C/day, associated with the mesoscale events. Under the influence of the intense mesoscale activity in deep winter, the upper layer becomes homogeneous as a result of vertical mixing, with relatively low temperatures (~13 °C) in both the coastal and central zones. From early spring, while the mesoscale activity is reduced, the stratification reappears.

This overview of the seasonal and mesoscale variabilities, from both the hydrological data and the current measurements, clearly indicates that two major "seasons" can be defined according to the dynamics of the Northern Current: a season when the mesoscale variability is especially intense and when the flux is maximum (~1.6 Sv), while the uns-

table current becomes narrower and deeper, flowing closer to the coast; and another season when the mesoscale variability is relatively weak and when the rather stable current is mainly wide and shallow, with flux values slowly decreasing (towards ~1 Sv). According to previous results (Taupier-Letage and Millot, 1986; Sammari *et al.*, 1995) in the northern Ligurian Sea, the mesoscale activity is relatively weak in spring-summer and starts to increase relatively rapidly in autumn, so that the most intense mesoscale activity tends to be limited to the winter. Our own results emphasize, at the beginning of the experiment, *i.e.* in early winter, an increase which starts with relatively high values, thus indicating that it has begun earlier, *i.e.* in autumn. This increase continues until the deep winter when the highest values are observed, and is followed by a rapid decrease in late winter. It is clear that our results are consistent with the previous ones. Therefore, as part of the two "seasons" defined above, the current time series have been halved from late December to mid-March, and from mid-March to late May; hereafter, for the sake of simplification, both seasons will be referred to as winter and spring, respectively. The statistical parameters presented in the following sections have been computed over both seasons.

BASIC STATISTICS

Standard deviation ellipses

The fluctuations of the Northern Current have first been classically investigated through the standard deviation ellipses (Ventsel, 1973), represented at all points with the mean currents on Figure 10, for both seasons; each semi-axis is equal to two standard deviations (2σ), hence 95 % of the measured currents are within the ellipse.

In winter (Fig. 10a), at each point, the ellipses at the upper levels are rather similar in both mean currents and principal axis directions, which confirms the occurrence of the upper layer already defined; the eccentricities are relatively low (0.5-0.7). At pts 2, 3 and 4, and mainly in this upper layer, the mean currents are generally southwestward and lower than 2σ. The large values of 2σ, mainly within the current (pts 2 and 3), show the large intensity of the mesoscale variability. Note the very low mean currents at pt 1 in winter, when this point is most of the time outside the current (see Fig. 9). Inside the current (pts 2 and 3) and at the upper levels, the major axis directions are quasi transverse to the mean flow, whereas more or less outside the current (as at pts 1 and 4) they are less transverse. Otherwise, they are strongly influenced by the topography at the deeper levels, where the larger eccentricities (~0.9) indicate that the fluctuations are mostly rectilinear. Close to the bottom, especially at P38 which clearly displays as expected a large ellipse compared to the one at P36, the major axis in the direction of the local isobaths and the large eccentricity (1.0) account for a flow strongly driven by the foot of the continental slope, acting as a wall.

In spring (Fig. 10b), the ellipses at each point are still similar in both mean currents and principal axis directions
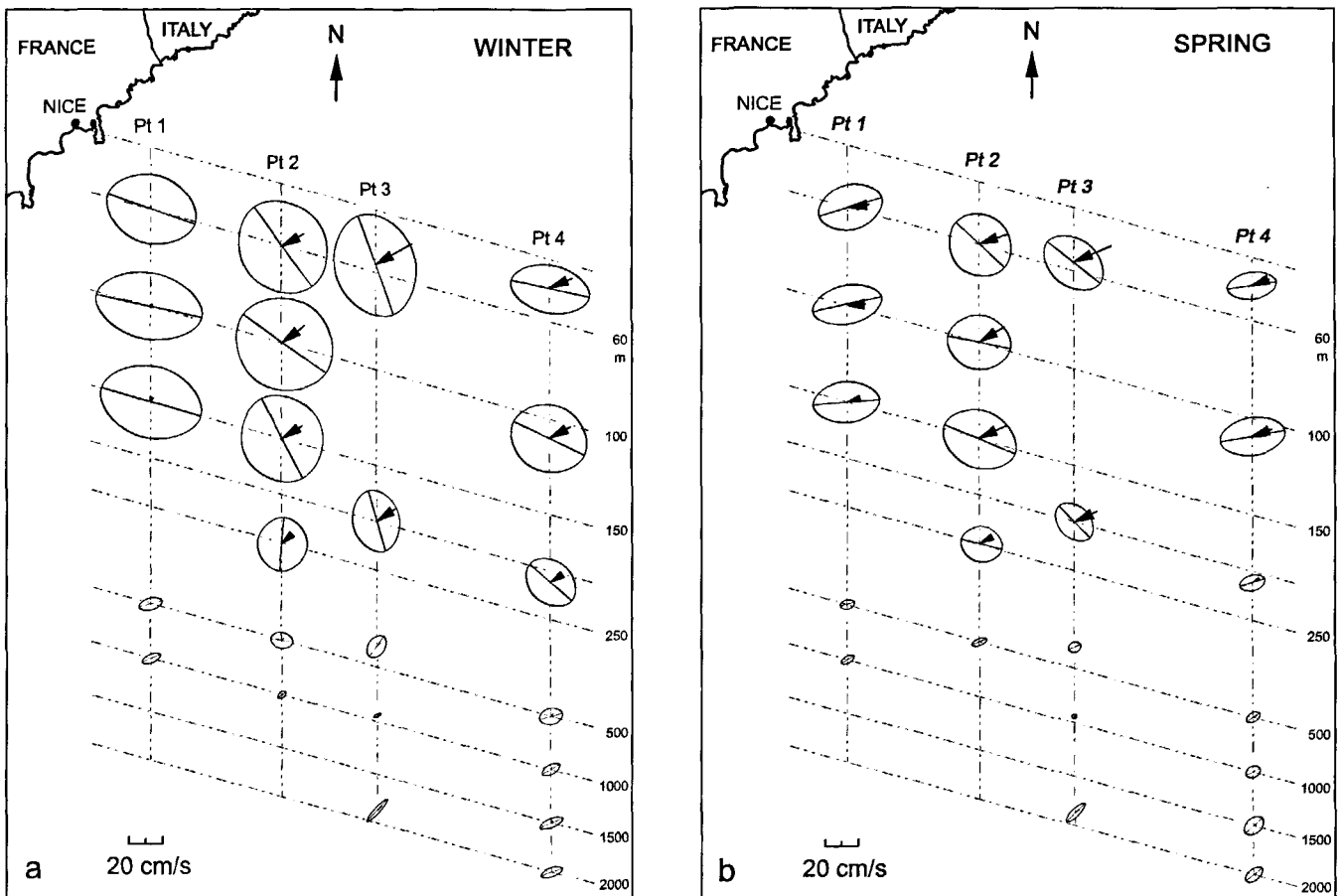
Figure 10

Standard deviation ellipses and mean currents at each point in winter (a) and spring (b). The length of the semi-axis is two standard deviations (95 % of the measured currents are within the ellipse).

in the upper layer. The eccentricities (0.6-0.8) are mostly a little larger than in winter, so that the fluctuations are in general more rectilinear. Within the current (mainly at pts 2 and 3), the principal axes are shorter (by ~30 %) than in winter and the mean southwestward currents are quasi equal to or larger than 2σ. Note that the mean flow at pt 1 is now much larger than in winter and also surface-intensified, mainly due to the brief period in early spring when the current has reached pt 1. At pts 2 and 3, the major axis directions are less transverse than in winter, while at pts 1 and 4, they are roughly parallel. The fluctuations at the deeper levels, mainly constrained by the topography, do not differ greatly from the winter ones, but are generally less intense.

The most interesting result of this analysis is that, in winter and within the core (pts 2, 3), the major fluctuations of the Northern Current occur mainly in a quasi transverse direction. Since the mesoscale variability is important, this might signify the occurrence of steep and large mesoscale meanders in winter. Conversely, on the inner (pt 1) and outer (pt 4) edges of the current, *i.e.* at some distance from the middle of the meanders, the directions of the fluctuations are more variable, so that the major axis directions are less significative. In spring, the mesoscale variability is reduced and the major axes are less transverse to the mean flow, accounting for a reduced instability. This is consis-

tent with previous analyses (Sammari *et al.*, 1995) which have emphasized fluctuations more parallel to the mean flow, resembling pulses between May and early autumn and then meanders until December. These results account for a continuous decrease, from winter to summer at least, of the mesoscale variability.

Integral time scales

Hereafter, the velocity of the current will be referred to a Cartesian coordinate system (x,y), with the x-axis oriented parallel to the mean flow (240° T), positive northeastward, and y-axis positive shoreward. We denote by u and v the alongshore and transverse components of the current, respectively.

The integral time scales have been estimated from the autocorrelation function (Sciremammano, 1979) as $\tau = (1 + 2\sum_{i=1}^{L}\rho_i^2)$. Δt where ρ_i is the correlation at lag i, Δ_t the data time interval and L the maximum lag used, chosen to be large enough compared to the lag number at which this function is statistically zero (usually ~20 % of the total record length, *i.e.* here ~29 days). The parameter τ provides information about the variability of the flow; it is also used to obtain the number of degrees of freedom n = $N\Delta t/\tau$ defined by Davis (1976), which corresponds to the

number of independent measurements used to estimate the significance level of a correlation value. Some significant differences have been emphasized, mainly according to the season and the location of the points (Albérola, 1994).

In winter, the alongshore and transverse fluctuations of the Northern Current have similar and relatively short time scales (generally 2-4 days), accounting for a large mesoscale variability in agreement with the former analyses and especially the standard deviation ellipses. The fluctuations support an unstable current that is mainly altered by instability processes leading to meanders.

In spring, the alongshore fluctuations have longer time scales (2-7 days) within the current and can be considered as pulses of a more stable flow, even if the transverse fluctuations persist at similar time scales as in winter. So, we can definitely say that alongshore pulses are predominant from spring until late summer, whereas fluctuations resembling meanders appear from autumn.

The temperature time scales (τ_T) evidence clear differences in the upper layer between winter and spring.

In winter, they clearly tend to lengthen with progress shoreward, ranging from 3-9 days on the outer edge (pt 4) to 15-18 days at the nearshore point (pt 1).

In spring, the horizontal differences are less apparent and in the upper layer (even to a depth of ~250 m), τ_T is shorter (1-10 days) than in winter. This is not surprising, as the overall temperature distribution is very different in both seasons. In winter, violent meteorological conditions induce an intense cooling of the central zone of the Northern Basin and thus a marked on-offshore temperature gradient; due to the occurrence of steep meanders, the temperature fluctuations (resp. time scales) will be very different from pts 1 to 4 and much rapid (resp. shorter) at the latter than at the former point. In spring, the on-offshore gradients are relatively smooth, the meanders are much less intense, and most of the fluctuations result from the large scale heterogeneity of the water masses transported by the Northern Current; the temperature fluctuations and the time scales will be roughly similar at all points.

Space correlations

Complex (Kundu, 1976) and scalar correlations have been computed between all pairs of Lanczos-filtered current time series, for both winter and spring and on both the vertical and the horizontal planes. As suggested by Sciremammano (1979), the raw correlations have been normalized by the large-lag standard error ($s^2=1/n$, n being the number of degrees of freedom) to permit comparison of time series having different time scales of variations. The detailed analysis is presented in Albérola (1994).

In both seasons and at all points, the highest correlations on the vertical are obtained in the upper layer with negligible time lags and rotations. Within this layer, the correlations between the points located at less than ~25 km from the coast are usually larger than those with pt 4 located further seaward. Therefore, there exists everywhere an upper layer which actually reacts like a slab, but significant differences occur on an on-offshore direction according to the season.

In winter, pt 4 is practically not correlated with the others (weak correlations, large time lags and rotations). In the coastal zone (width generally < 25 km), the fluctuations (especially the transverse ones) are very well correlated on both the vertical and horizontal planes down to ~500 m. Seaward from ~25 km, both transverse and alongshore fluctuations are strongly correlated roughly throughout the whole depth, with clear indications that the mesoscale events there are the intense and rather barotropic ones of the central zone. These results evidence the narrowness of the Northern Current in winter, the outer edge being at less than ~25 km, as well as the occurrence of steep meanders due to the large instability. They also emphasize the extension of the central zone and confirm the growth of intense barotropic mesoscale phenomena.

In spring, there are some significant correlations between pt 4 and the other ones in the upper layer. This accounts for a Northern Current that is wider than in winter and generally covers the whole studied area. In the coastal zone (width generally > 25 km), the transverse and alongshore fluctuations show slightly less correlation than in winter throughout the upper layer; the highest correlations are computed within the core, indicating that these fluctuations might be linked to less steep meanders or phenomena resembling pulses of the current. Seaward from ~25 km, the vertical correlations are not as significantly deep as in winter, accounting for the disappearance of the barotropic mesoscale phenomena there and thus indicating that the central zone does not extend as far shoreward as in the deep winter.

EMPIRICAL ORTHOGONAL DECOMPOSITIONS

The Empirical Orthogonal Functions (EOF) decomposition, as formulated by Wallace and Dickinson (1972), transforms a data set into a set of statistically independent modes and has been extended to a group of vector time series by Kundu and Allen (1976). These techniques have been applied to the set of 20 time series for which the total length was available (*i.e.* except P11, P12 and P26); these time series with their mean removed have been analysed per mooring, per level (in detail in Albérola, 1994), and collectively *i.e.* on a vertical plane transverse to the mean current.

Vertical and horizontal structures from EOF

At each point, a single complex EOF (Fig. 11), similar to a barotropic mode, given the few varying directions of the eigenvectors with depth, contains ~94 to 80 % of the variance with a monotone decrease in a seaward direction; the second mode (not shown) has the shape of a first baroclinic mode and accounts for less than 10 % of the variance. In the upper layer, the eigenvectors at each point are very similar in both amplitude and direction; note that they maintain their similar direction as deep as 500 m, even if
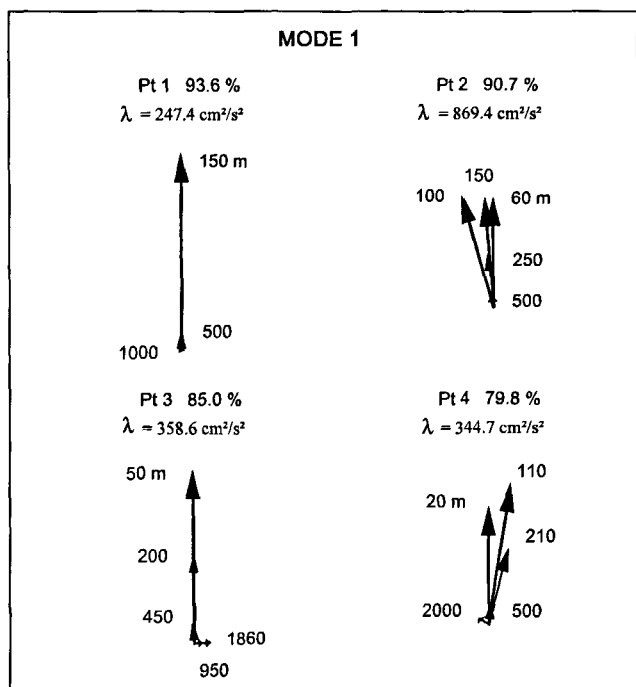
MODE 1

| Pt 1 93.6 % | Pt 2 90.7 % |
| $\lambda = 247.4$ cm²/s² | $\lambda = 869.4$ cm²/s² |

| Pt 3 85.0 % | Pt 4 79.8 % |
| $\lambda = 358.6$ cm²/s² | $\lambda = 344.7$ cm²/s² |

Figure 11

First complex empirical orthogonal mode at each point. The vectors are relative to the shallowest one which is oriented upwards. The percentage of total energy is indicated as well as the eigenvalues λ (cm²/s²).

they then have a smaller amplitude. This signifies similar current fluctuations at each point throughout the upper layer, as expected from the analyses described above, and supports the vertical extent of the mesoscale events which appear to have a rather simple vertical structure, displaying quasi no rotation with depth.

The complex EOF decompositions at each level (not shown) emphasize that the first mode is strongly correlated with the points within the current for which it explains 76-98 % of the variance. Conversely, the second mode is mainly governed by the variability at pt 4, with 72-95 % of the variance explained in comparison with only 2-15 % at the other points. Thus, considered as a whole, the dynamic structure at pt 4 is actually different and more complex than at the other points because, due to the variations of the Northern Current in width and depth, this point is located either outside or more or less inside the current.

Transverse section of the Northern Current from EOF

Such a decomposition is expected to give a description of the major fluctuations of the Northern Current which are coherent over most of the network; only the first mode is presented. The amplitude factors of the first mode for both components are represented in Figure 12; this mode explains 57 % of the total variance for the u component (Fig. 12*a*), which is relatively low, and 74 % for the v component (Fig. 12*b*). The maximum values are found within 10-15 km for the u component and 15-20 km for the v component, *i.e.* rather within the core of the current for both components; the amplitudes are even higher for v than for u. The shape of the alongshore fluctuations clearly

indicates that the outer edge of the current is for the greater part of the time located at ~25 km from the coast and that the currents outside the vein are not very significant. This supports the location of pt 4 in a regime which often differs from that at the other points, as just depicted and already observed on the vertical sections of the geostrophic current (Fig. 3*b*). The maximum amplitudes, found within the core of the current for the v component, confirm the importance of the transverse fluctuations and indicate their shape through quasi horizontal isolines, spreading over the whole width of the current and down to ~500 m. These transverse fluctuations should be considered as meanders generated by an unstable flow, and support the analysis of the standard deviation ellipses (Fig. 10) as well as that derived from the correlation functions (section 3). The PROLIG-2 observations have evidenced that, from late spring to autumn, the transverse fluctuations are strongest not in the core of the current but on the inner edge (Sammari *et al.*, 1995); moreover, the first mode of a similar EOF decomposition, performed over a set of 9 records, explains ~83 and 74 % of the total variance for the u and v components, respectively. Therefore, our results account
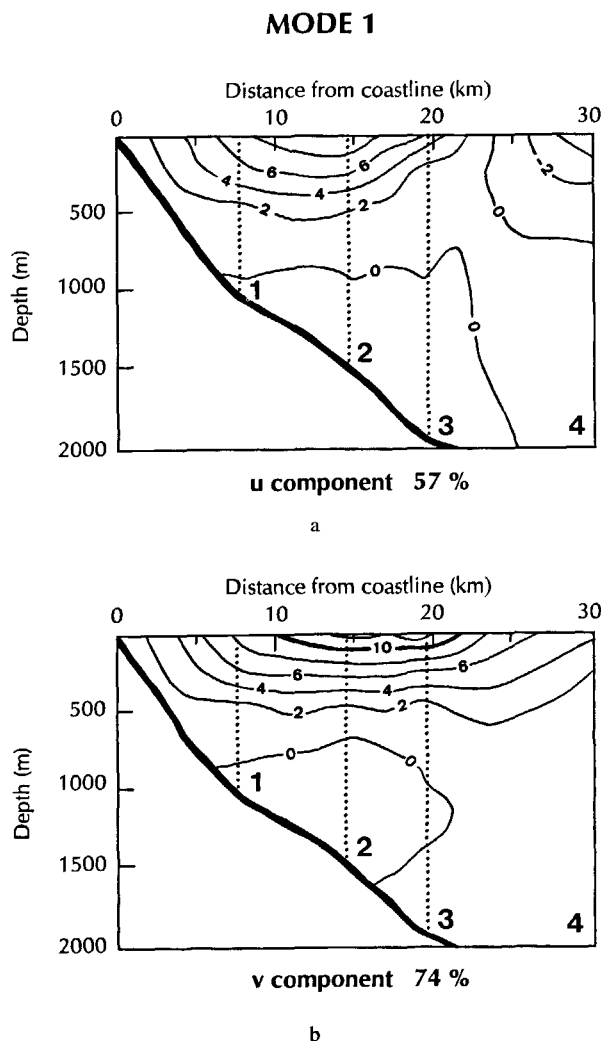
MODE 1

u component 57 %

a

v component 74 %

b

Figure 12

Amplitude factors of the first empirical orthogonal function, using the whole 20 time series, for the u (a) and v (b) components. Locations of the mooring points are indicated by dotted lines.

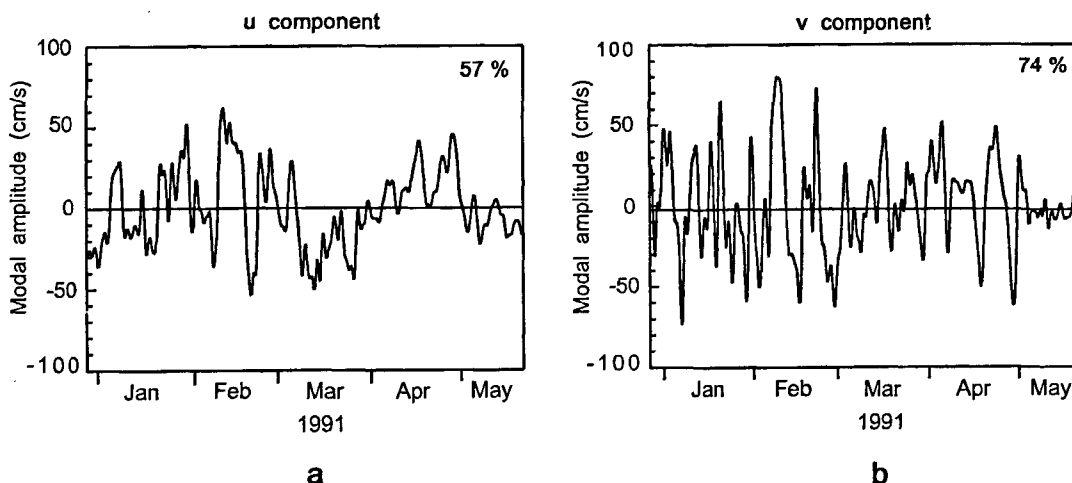## MODE 1

u component

v component

57 %

74 %

a

b

Figure 13

Modal amplitudes E_u (a) and E_v (b) of the fluctuations of each component (Δt is 6 h) in the first empirical orthogonal mode, using the whole 20 time series. The percentage of the total variance explained by this mode is indicated.

for a more complex structure, and it is clear that the Northern Current can be strongly modified by dramatic winter processes.

The modal amplitudes (E_u, E_v) of the first mode of this decomposition are presented for both components in Figure 13. From a visual examination, E_u displays fluctuations at 10-15 days while E_v fluctuates mainly at ~10 days; shorter fluctuations are observed mainly on E_v. This will be specified in the following section.

Dynamic modes

The velocity field can be decomposed into its dynamic modes, determined by the solutions of the simplified equa-

tions of motion (Kundu *et al.*, 1975), in order to evidence the nature of the fluctuations of the current by estimating the relative strengths of each mode. The Brunt-Väisälä frequency N(z) (z being the depth) is an input parameter of the problem and mean N(z) profiles have been deduced, for each season, from mean density profiles computed by using the hydrological data collected during the period of the current measurements. The boundary conditions, based on several approximations, include a flat bottom so that, given the relatively homogeneous characteristics generally observed deeper than ~700 m, the mean N(z) profiles have been extrapolated down to 2000 m. The vertical profiles of the first three modes are represented in Figure 14, for both seasons.
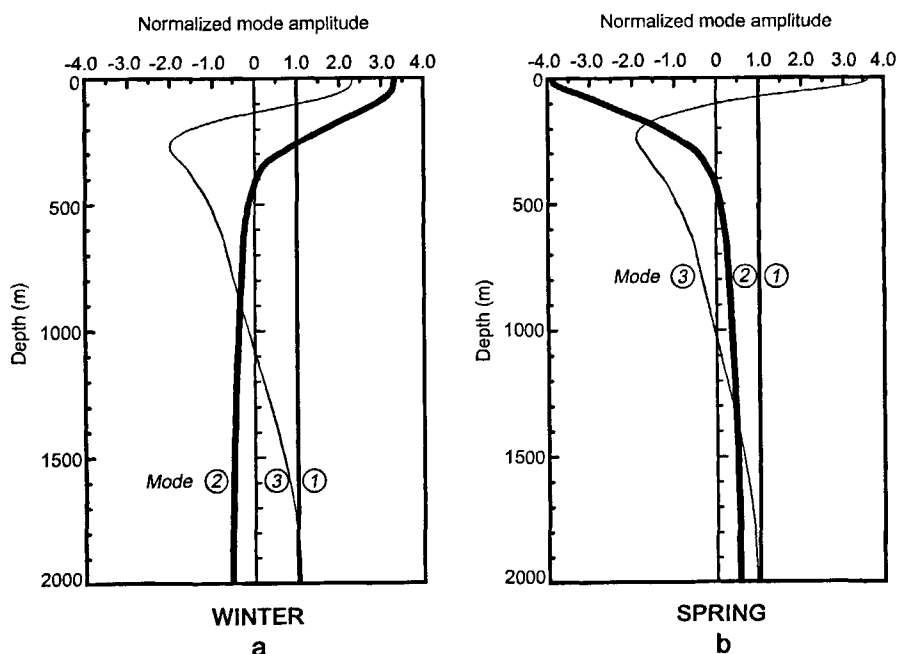
Normalized mode amplitude

Normalized mode amplitude

Mode ③

Mode ② ③ ①

WINTER

a

SPRING

b

Figure 14

Vertical profiles of the first three dynamic modes in winter (a) and spring (b).

In winter (Fig. 14a) and in the upper layers, the zero-crossings of the baroclinic modes are situated at ~400 m for the first and ~130 m for the second, while in spring (Fig. 14b), they are slightly deeper (~430 m) and shallower (~100 m), respectively, and more surface-intensified. The sum of the barotropic and first baroclinic components has been computed for comparison with the measured alongshore component; Figure 15 shows the results obtained at P21, as an example. Note that the measured current is relatively well represented by these first two modes. Similar results are obtained throughout the upper layer and the residual left after fitting the computed to the measured current begins to increase from ~250 m; the overall residual (time and depth average of the residual from 60 down to 500 m) is 20-25 % in both seasons (similar values are obtained at pt 3 between 50 and 1860 m). In both seasons and in the upper layers, the energy of the barotropic mode, at each depth, accounts for ~5 to 10 % of the energy of the alongshore component, whereas the energy of the baroclinic component is greater in winter (40-90 %) than in spring (15-75 %), irrespective of the depth.

These analyses emphasize that the current can be relatively well represented by the barotropic and first baroclinic components, which are the predominant modes, the other modes and the residual being contained in only 20-25 %. In the upper layers, the baroclinic mode is clearly more energetic than the barotropic one. Its zero-crossing at 400-500 m indicates that the mesoscale events, generally observed down to these depths and often weakening with depth, probably have a structure resulting from the sum of both the first baroclinic mode and the barotropic mode which compensates the baroclinic one at depth. This agrees with the EOF decomposition showing quasi no rotation of the fluctuations with depth, as deep as ~500 m.

SPECTRAL ANALYSIS

Both scalar and rotary (Gonella, 1972) spectra have been calculated over both seasons and are presented in an energy-preserving form (Dickson, 1983), using frequency-averaging. The advantage of such a representation is that the energy content, in each period band, is immediately appreciated when comparing the points or the different depths, for both components or for the clockwise/anticlockwise energy. All the period bands (a total of 9) have been selected according to the full spectra of the hourly time series, for each depth and season. The estimated number of degrees of freedom (period band in days) is 28 (1.5-2.5), 10 (2.5-3, 3-3.5, 3.5-4.5) and 6 (4.5-6, 6-8, 8-12, 12-22, 22-74).

As expected from all the previous analyses of the time series, both scalar and rotary spectra are similar at each point throughout the upper layer, so that only representative spectra (at the 100-m level at pts 2 and 4, 50-m level at pt 3 and 150-m level at pt 1) have been plotted in Figures 16 and 17 for both seasons. It will be shown that specific fluctuations occur in the 8-22 day period band with, under certain conditions, more energy at 8-12 days, so that for the sake of simplicity, we will deal below with a 10-20 day band with a possible predominance at ~10 days. Another specific period band will be the 3-6 day one.

Scalar spectra

In winter (Fig. 16), the u-spectra show that most of the energy is contained in the 10-20 day band, with rather similar values at each point. At pt 1, on the inner edge of the current or in the coastal zone, the alongshore fluctuations occur mainly at ~10 days. The v-spectra indicate

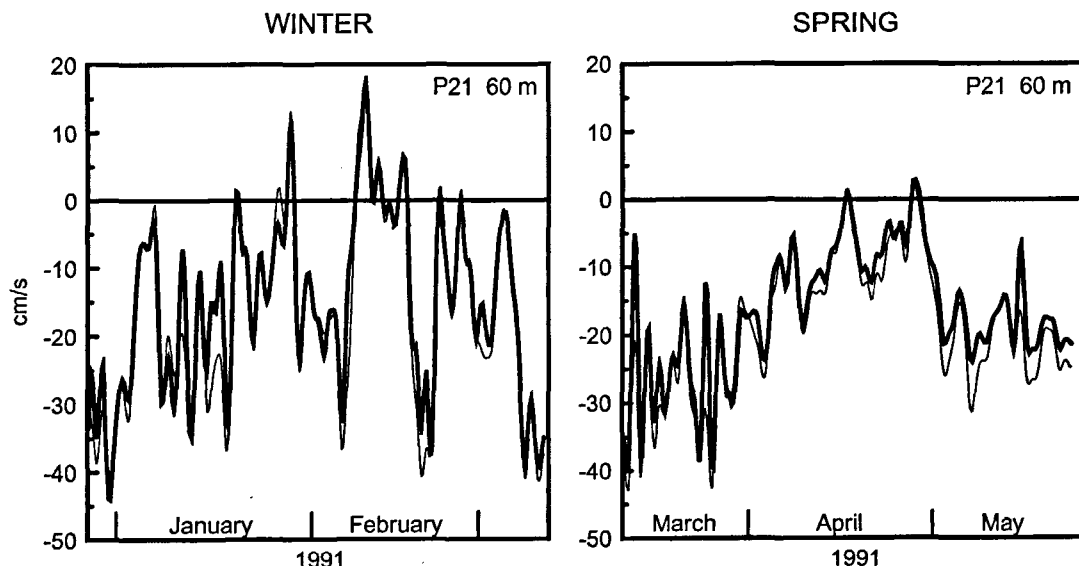WINTER   SPRING

Figure 15

Sum of the barotropic and first baroclinic components (thin line) and alongshore component (heavy line) of the P21 time series.

the same period band with an energy content varying according to the location of the points. Within the current (pt 2 and mainly pt 3), the transverse fluctuations in the 10-20 day band are clearly more energetic than the along-shore ones and the peak is maximum at ~20 km from the coast (pt 3). On the inner edge (pt 1), the transverse fluctuations occur preferentially at ~10 days, like the along-shore ones, probably signifying that the main mesoscale phenomena have slightly shorter periods on the inner edge than within the core. On the outer edge (pt 4), the energy content for the transverse fluctuations in the 10-20 day band is lower than close to the core (pts 2, 3). These results are coherent with the occurrence of meanders as emphasized by the standard deviation ellipses, since the transverse fluctuations are very important within and close to the core of the current, whereas fluctuations more in the direction of the mean flow occur on the edges. The trans-verse fluctuations also occur at shorter ~3-6 day periods, which is coherent with previous observations (Sammari et al., 1995). Such fluctuations are more clearly observed at pts 2 and 3 and thus appear to be more characteristic of the core of the current than of its edges.

In spring (Fig. 16), the energy content in each period band is clearly lower than in winter, due to the relatively weak mesoscale activity. The u-spectra are less energetic and no period band is clearly predominant, except at pt 4 where the alongshore fluctuations are still persistent at ~10 days. Note that the maximum 10-day peak observed in winter at pt 1 has collapsed together with the mesoscale activity (Fig. 8), so that the two phenomena might be rela-ted, signifying that the mesoscale activity occurs mainly at ~10 days. The v-spectra are more energetic than the u-ones. The transverse fluctuations occur now at ~10 days, indicating that the 10-20 day band has reduced. The most energetic peaks are still obtained within the current (pts 2 and 3), signifying the persistence of meanders in spring even if they are less energetic than in winter. On the inner edge, no predominant period of these fluctuations is clear-ly defined, partly due to the shorter record length at P11 and P12 (not shown), but mainly due to the location close to the coast; even the P13 spectrum, with actually very little energy, does not emphasize any clear period for the transverse fluctuations. The transverse fluctuations in the 3-6 day period band are still observed, here again more at pts 2 and 3 than at the other points, but they are also clear-ly less energetic than in winter. This result is in good agreement with previous ones (Sammari et al., 1995) which have shown that such relatively rapid fluctuations, involving little energy in spring-summer, became energe-tic from autumn. In general, the fluctuations of the Nor-thern Current appear to have shorter periods in spring than in winter, since the 10-20 day band is reduced to ~10 days.

Below the upper layer (not shown), the energy widely decreases with depth and as a general rule, even if it is not very pronoun-ced, there is more energy in the u- than in the v- spectra.

In winter, the 10-20 day band is still observed at pt 2 down to ~500 m for both components, while the alongshore fluc-tuations occur preferentially at ~10 days on the outer edge of the current (pt 4) down to ~1500 m and at pt 3 down to ~500 m.

In spring, the energy content is very small, but the 10-20 day band persists for the u component at the deepest levels. Concerning the topographic effect induced by the foot of the continental slope, the P38 spectrum displays alongshore fluc-tuations which are very energetic in comparison with the flat P36 spectrum, at ~10 days and with a cascading energy to the short periods in winter, and mainly at 10-20 days in spring.

Therefore, the scalar spectra indicate that in winter, both alongshore and transverse fluctuations occur within a main 10-20 day period band. If the alongshore fluctuations can be depicted as pulses of the Northern Current, the most energe-tic transverse fluctuations, observed within its core, account for the occurrence of meanders and are coherent with the results obtained from the standard deviation ellipses. The signature of meanders is still emphasized in spring by the persistent transverse fluctuations within the current. They have periods slightly shorter than in winter, the 10-20 day band being reduced to ~10 days. In both seasons, the trans-verse fluctuations also occur at relatively short periods in the 3-6 day period band, and seem to be characteristic of the core of the current. The mesoscale phenomena at pt 1 have periods at ~10 days slightly shorter than those observed within the current (pts 2, 3). This is in agreement with the fact that pt 1 has been observed most of the time outside the current or rather on its inner edge; hence some fluctuations might be specific to this location and might sometimes occur simultaneously with those generated by the current itself when it flows closer to the coast. The transverse fluc-tuations are actually important and may play a crucial role in the dynamic transformations of the Northern Current. If they have already been observed at short periods, the longer periods observed in winter were rather unexpected.

Rotary spectra

From Figure 17, it may be seem that the energy polariza-tion varies clearly according to the location of the points.

In winter, the anticlockwise energy is relatively low on the inner edge (pt 1), spreading from ~10 days to the short periods. When progressing seaward, it appears at 3-6 days at pts 2 and 3, and reaches a maximum at ~10 days at the latter point. On the outer edge (pt 4), most of this energy is contained at longer periods well within the 10-20 day band. These observations might indicate that two kinds of mesoscale phenomena, one having relatively short periods in the 3-6 day band and the other having longer periods at 10-20 days, often occur simultaneously. The clockwise energy is clearly maximum at ~10 days at less than 10 km (pt 1) and decreases seaward, the axis of the current being expected between 15-20 km (pts 2-3) from the coast where both kinds of energy are equally shared. The clockwise energy interests roughly a broader 5-20 day band at pts 2 and 3, while it is especially low at pt 4. The main fea-ture is hence that, in the seaward direction, the anticlock-wise energy increases while the clockwise energy decreases: this is a clear signature of the occurrence of meanders.
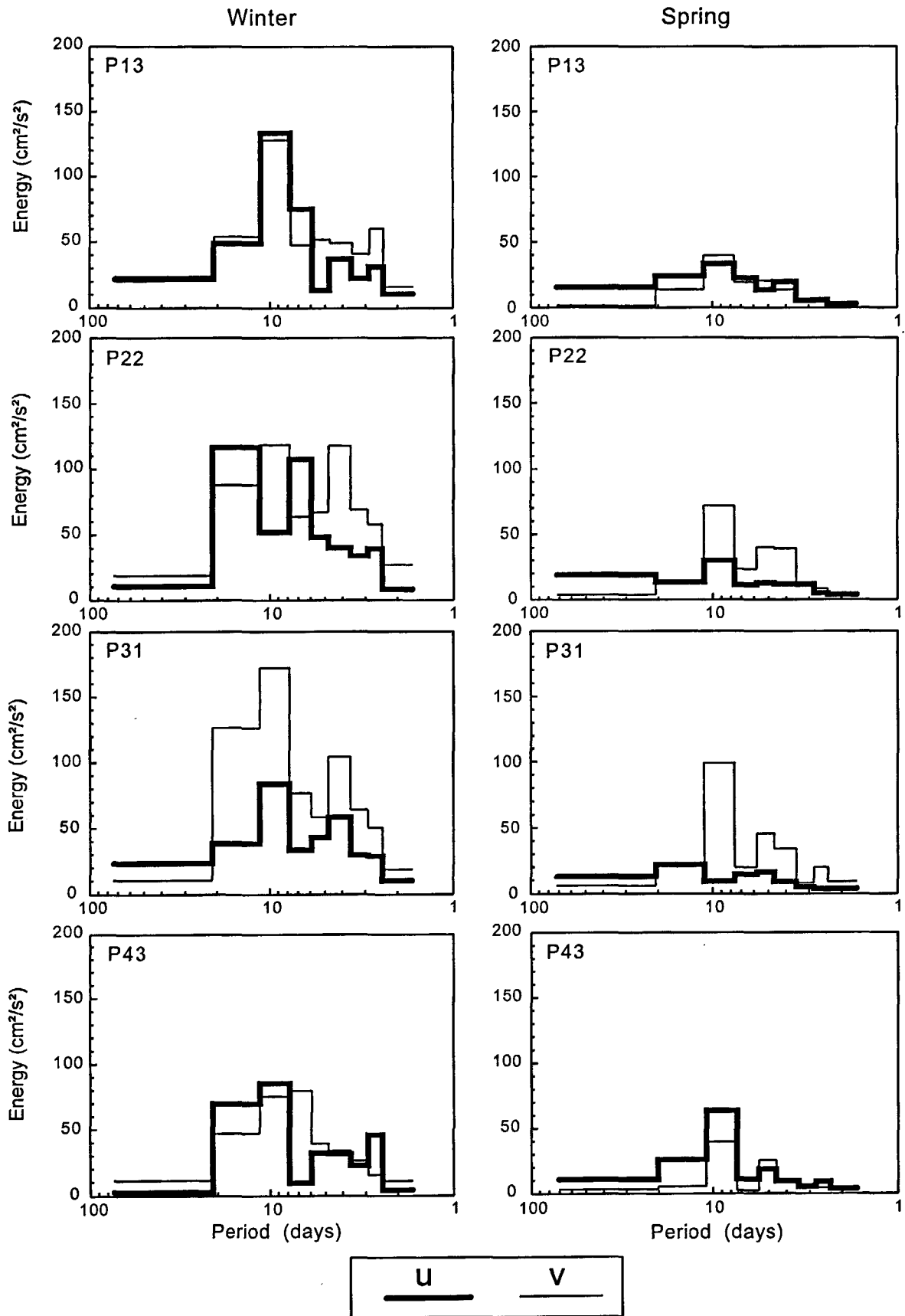
Figure 16

Scalar spectra representative of the upper layer, at each point and for both seasons, presented in an energy-preserving form. The number of degrees of freedom for each period band is indicated in the text.
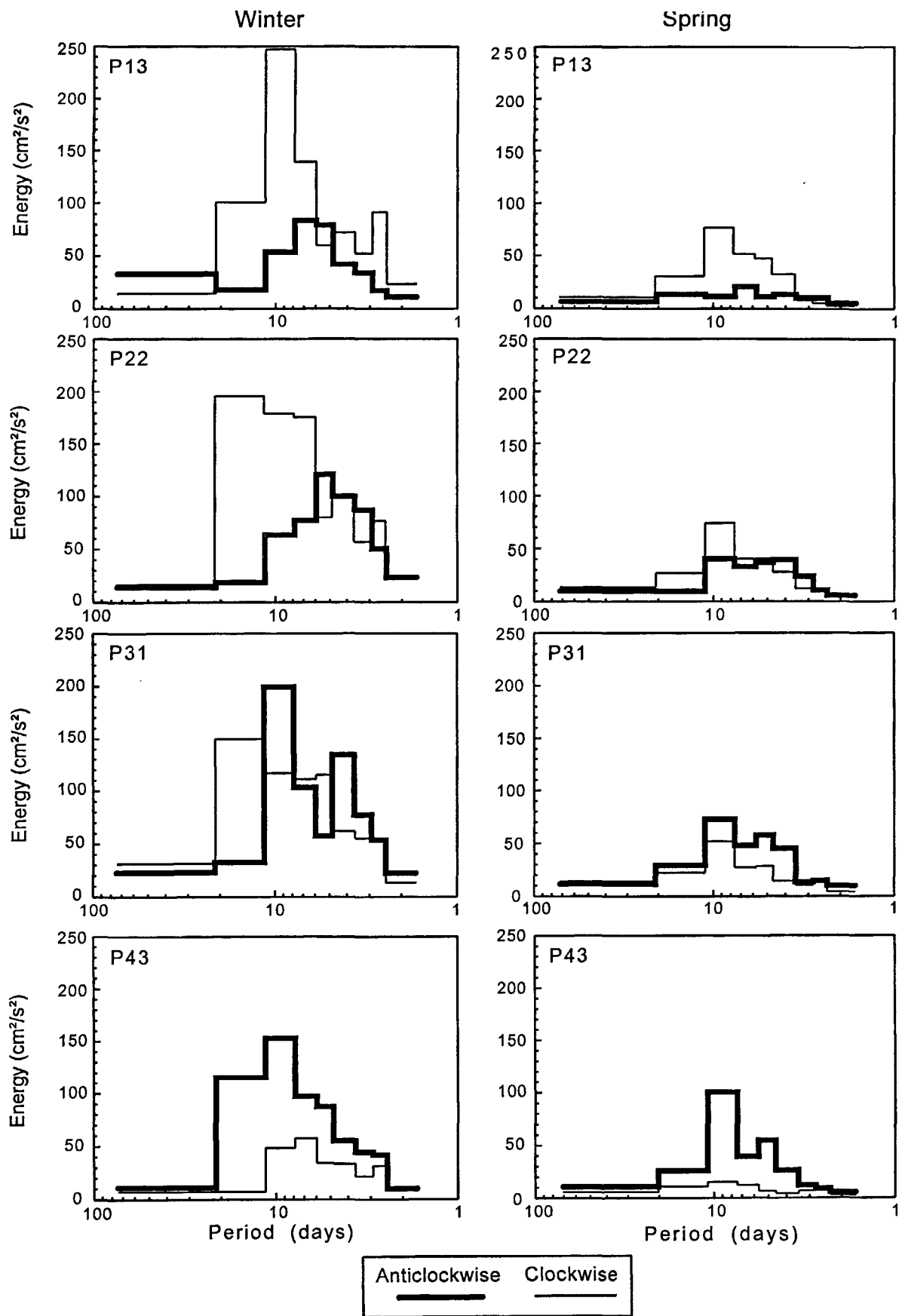
Figure 17

Rotary spectra representative of the upper layer, at each point and for both seasons, presented in an energy-preserving form. The number of degrees of freedom for each period band is indicated in the text.

In spring, the spectra are less energetic than in winter. However, the anticlockwise energy continues to increase while the clockwise energy fades with progress seaward. This means that, although they are clearly less energetic than in winter, the meanders are persistent in spring, as deduced from the scalar spectra of the transverse fluctuations. The **anticlockwise energy** displays a flat spectrum at pt 1 and begins to rise at pt 2 at periods shorter than 10 days; it remains predominant from the core of the current (pt 3) to the outer edge (pt 4), mainly at ~10 days. The **clockwise energy** appears mainly at pt 1, at periods similar to the winter ones, and at pts 2 and 3 where the broad 5-20 day band has now reduced towards the shorter periods. This supports the thesis that the mesoscale phenomena have slightly shorter periods in spring than in winter, in agreement with the scalar spectra. The flat spectrum observed at pt 4 accounts significantly for the seaward decrease of the clockwise energy.

At the deeper levels (not shown), although the spectra are less energetic, some differences appear between both polarizations.

In winter, the clockwise energy is generally preponderant in the 10-20 day band, except at pt 3; the energy at pt 3, in the same period band, is polarized in the anticlockwise direction.

In spring, both kinds of energy fade and there are no clear signals. Nevertheless, the fluctuations at P38, sustained by the topographic effect, appear at ~10 days in winter and more or less at slightly longer periods in spring, while the P36 spectra are quite flat for both seasons.

Especially noteworthy is the fact that the Northern Current clearly appears as a meandering current whose anticlockwise energy increases with progress seaward, while the clockwise energy vanishes. The meanders are widely energetic in winter, due to the especially intense mesoscale activity which obviously involves much more energy in the winter processes than in the spring ones. Nevertheless, the meanders are still persistent in spring at slightly shorter periods.

Vertical and horizontal coherences

From the vertical and horizontal coherences calculated in the upper layer (Albérola, 1994), in an attempt to estimate the space scales of the fluctuations of the Northern Current, some main features can be confirmed. The alongshore fluctuations are mostly not coherent in winter, due to the widely energetic meanders. In spring, they are coherent mainly at 10-20 days, supporting the occurrence of pulses, to which they have already been compared. The transverse fluctuations in the same band are in general vertically well coherent over at least the whole upper layer. This is in agreement with a vertical extent of a few hundred metres, as expected from previous analyses (stick-diagrams, standard deviation ellipses, correlations, spectra). The transverse fluctuations might be actually intense in winter to interest the major part of the vein. They are more coherent between neighbouring points *i.e.* over some few kilometres, hence they might propagate while their energy fades. The transverse fluctuations at 3-6 days are significantly coherent within the current, signifying a relatively small horizontal extent.

Spectra of the modal amplitudes

Spectral analysis has been performed over the modal amplitudes (E_u, E_v) of the EOF decomposition using the entire 20 time series (§ Transverse section of the Northern Current from EOF; Fig. 13), for both seasons; the spectra are plotted in Figure 18. The spectra of such amplitudes are supposed to indicate only the period band of the most coherent fluctuations over the network. From Figure 18, the coherent alongshore fluctuations actually occur in the 10-20 day period band in both seasons, indicating that the pulses of the Northern Current might have a horizontal extent of a few tens of kilometres. The coherent transverse fluctuations in the same band appear to occur rather at ~10 days in spring, in agreement with the fact that the mesoscale phenomena have periods slightly shorter than in
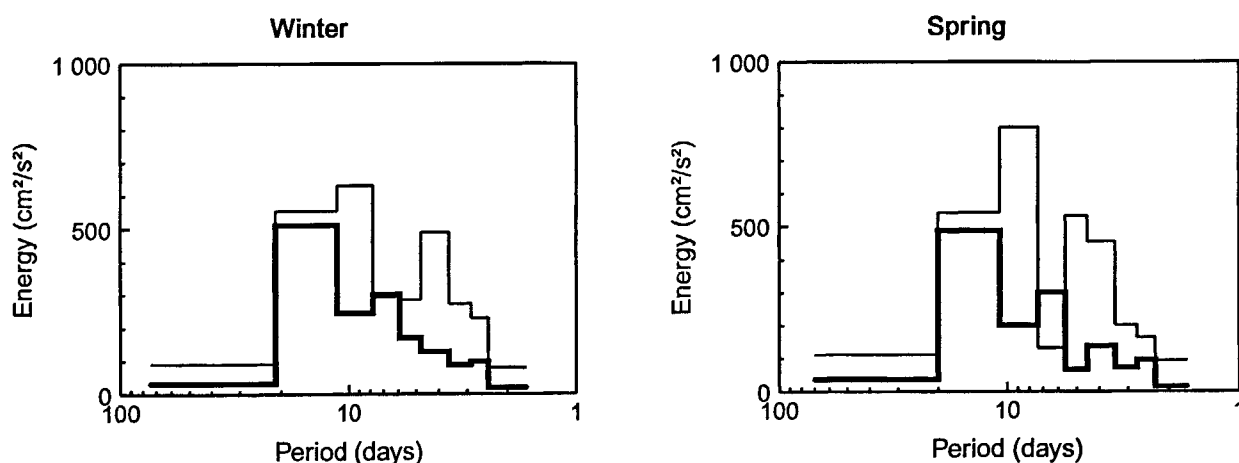

Figure 18

Scalar spectra of the modal amplitudes E_u (heavy line) and E_v (thin line) of the fluctuations, obtained from the EOF decomposition using the whole 20 time series.

winter. The short transverse fluctuations at 3-6 days, cha-racteristic of the core of the current where the modal amplitudes are maximum (Fig. 12), appear to be clearly coherent.

SUMMARY AND DISCUSSION

Thanks to the effort made during the PRIMO-0 experi-ment in the Ligurian Sea to collect hydrological data twice monthly over a period of 10 months and simulta-neous current measurements during 5 months, in both cases with relatively fine space scales, these observations have allowed us to shed more light on some of the main features of the seasonal and mesoscale variabilities of the circulation. Nevertheless, this sampling clearly remains rather rough with respect to the mesoscale variability, which could not be resolved. This shortcoming has pre-vented us from definitely differentiating the mesoscale and seasonal variabilities.

The Northern Current has been depicted from the entire set of observations as generally wide (> 30 km) and shallow (isotach 10 cm/s smooth and shallower than 200 m), with a well-defined episode of narrowing (< 20 km), deepening (isotach 10 cm/s steep and deeper than 200 m) and shore-ward shift from late January to mid-March. The hydrologi-cal characteristics of the different water masses have allo-wed us to follow their seasonal variations, principally with reference to the seaward spreading of LIW at the same time as the formation of WMDW, the formation of WIW in deep winter and the advection of less modified MAW. Due to a fine vertical resolution, currents have clearly appeared to be similar in an upper layer at least between 60 and 150 m, in both seasons, irrespective of the location of the points; this upper layer is expected to extend up to the surface. The flux of the Northern Current (between 0 and 300 dbar) has ranged within 1-1.6 Sv and its tempo-ral evolution has provided evidence of a rather long winter season when relatively high values are maintained. The flux is maximum (~1.6 Sv) in December and slowly decreases at least until July (~1 Sv). No significant seaso-nal variations of the flux have been evidenced between summer and early autumn from previous data sets. Our results concerning the flux are consistent with those repor-ted earlier, but the complexity and variability of the struc-ture of the current have underscored the importance of the kind of data (hydrological/current measurements) used in the estimation of the flux. Observations in the near coastal zone (of ~10 km) have shown that, except during the brief shoreward shift of the Northern Current, no mean circula-tion is observed there, while turbulences are predominant; this is of fundamental interest to coastal oceanography, the tasks of which are by no means facilitated by such an unforeseeable circulation. It should be noted that even if the mesoscale variability is large, seasonal variability has clearly appeared and thus has to be considered as actually important.

Mesoscale activity increases very rapidly from the begin-ning of the experiment until deep winter, shows a rapid

decrease in late winter and then has relatively small values, as already shown. It is known from earlier obser-vations that the mesoscale activity is relatively weak in spring-summer and starts to increase from autumn; this is coherent with our results, accounting for a continuous decrease of the mesoscale variability from winter to sum-mer at least. It has been clearly observed that the mesos-cale activity propagates to the open sea in deep winter. The mesoscale events are often intense enough to affect the whole width of the current, usually to depths of a few hundred metres, or even throughout the entire water column at the more seaward point when the occasional narrowness and shoreward shift of the Northern Current allow the barotropic structure of the central zone to spread shoreward.

In winter, the alongshore and transverse fluctuations of the current have large and similar amplitudes and relati-vely short time scales, suggesting a large mesoscale variability.

In spring, fluctuations of both kinds have smaller ampli-tudes and the alongshore ones have longer time scales than before, due to a reduced instability.

We have observed that both alongshore and transverse fluctuations occur in a main 10-20 day period band. One of our most interesting findings is that the major fluctua-tions of the Northern Current, generally quasi transverse within its core, account for a very unstable current mainly altered by instability processes, leading to steep and large mesoscale meanders. The polarization of energy is highly indicative of the occurrence of meanders since, when pro-gressing seaward, the anticlockwise energy increases while the clockwise energy vanishes.

In winter, these meanders are very energetic.

In spring, they are still persistent and are characterized by slightly shorter periods, the 10-20 days band having been observed to reduce to ~10 days. Despite this persistent meandering, the alongshore fluctuations are then predomi-nant and have been depicted as resembling pulses of a more stable flow. In both winter and spring, the transverse fluctuations also occur at relatively short periods in the 3-6 day band and have been observed preferentially within the core of the current. Such fluctuations might be the signature of meanders; however, since the 3-6 day band is not clearly apparent for the alongshore component on the edges of the current, these meanders are likely to have amplitudes smaller than those occurring at 10-20 days. Moreover, such meanders have been previously observed as intensifying between spring-summer and autumn, pro-pagating downstream at ~10 km/day. Our own findings, and especially the relatively high levels of energy obser-ved in winter with respect to spring for the transverse fluc-tuations at 3-6 days, lead us to suggest that this intensifica-tion continues in winter, being maximum in deep winter together with the mesoscale activity.

In the coastal zone over ~10 km, the main mesoscale phe-nomena have appeared at ~10 days, indicating periods slightly shorter than within the current. The overview of our observations in this zone leads us to expect that the predominant turbulences, characteristic of this coastal

location, might occur simultaneously with the major fluctuations of the current, especially when it flows close to the coast. Moreover, the continental slope acts as an inclined and rough boundary, so that the turbulences, probably generated by the current itself through, for instance, instability processes, may be expected to settle with progress shoreward, sustained by stronger and stronger interactions between the topography and the relatively deep vein formed by the Northern Current.

Some main features, emphasized in this overview of the mesoscale and seasonal variabilities of the Northern Current seem to be favourable to relationships between the circulation and the winter dense water formation, as suggested by models. Indeed, the dynamic regime at our most seaward point (~30 km), which in deep winter constitutes the barotropic regime of the central zone and accounts for an extension of this zone, together with the occasional narrowness and shoreward shift of the current as well as its relatively high flux values maintained during a rather long winter season, corresponding to the dense water formation season, might support such relationships between the advective and convective phenomena. Therefore, it would appear that in further experimental and theoretical investigations of the major forcings that drive the circulation in the northern part of the western Mediterranean Sea, winter dense water formation should be considered as playing one of the major roles.

REFERENCES

Albérola C. (1994). Contribution à l'étude des variabilités saisonnière et à méso-échelle de la circulation générale dans le nord de la Méditerranée occidentale. Thèse de Doctorat de l'Université Aix-Marseille II, 196 p.

Astraldi M., G.P. Gasparini, G.M.R. Manzella and T.S. Hopkins (1990). Temporal variability of currents in the eastern Ligurian Sea. *J. Geophys. Res.* 95, C2, 1515-1522.

Astraldi M. and G.P. Gasparini (1992). Seasonal characteristics of the circulation in the western Mediterranean basin and their relationships with the atmospheric-climatic conditions. *J. Geophys. Res.* 97, C6, 9531-9540.

Béthoux J.P., L. Prieur and F. Nyffeler (1982). The water circulation in the north-western Mediterranean sea, its relations with wind and atmospheric pressure. In: Hydrodynamics of semi-enclosed seas, J. C. J. Nihoul ed. 129-142.

Béthoux J.P., L. Prieur and J.H. Bong (1988). Le courant Ligure au large de Nice. *Oceanologica Acta.* Sp. issue, 9, 59-67.

Crépon M., L. Wald and J.M. Monget (1982). Low-frequency waves in the Ligurian Sea during December 1977. *J. Phys. Oceanogr.* 87, 595-600.

Crépon M. and M. Boukthir (1987). Effect of deep water formation on the circulation of the Ligurian Sea. *Annales Geophysicae* 5B, 1, 43-48.

Davis R. E. (1976). Predictability of sea surface temperature and sea level pressure anomalies over the North Pacific Ocean. *J. Phys. Oceanogr.* 6, 249-266

Dickson R.R. (1983). Global summaries and intercomparisons: flow statistics from long-term current meter moorings. In "Eddies in Marine Science", A.R. Robinson Ed., Springer-Verlag, 278-328.

Font J., J. Salat and J. Tintoré (1988). Permanent features of the general circulation in the Catalan Sea. *Oceanologica Acta*, Sp. issue, 9, 51-57.

Font J. (1990). A comparison of seasonal winds with currents on the continental slope of the Catalan Sea (northwestern Mediterranean). *J. Geophys. Res.* 95, 1537-1545.

Gascard J.C. (1978). Mediterranean deep water formation, baroclinic instability and oceanic eddies. *Oceanologica Acta*, 1, 3, 315-330.

Gonella J. (1972). A rotary-component method of analysing meteorological and oceanographic vector series. *Deep Sea Res.* 19, 833-846.

Kundu P.K., J.S. Allen and R.L. Smith (1975). Modal decomposition of the velocity field near the Oregon coast. *J. Phys. Oceanogr.* 5, 683-704.

Kundu P.K. (1976). A note on the Ekman veering observed near the ocean bottom. *J. Phys. Oceanogr.* 6, 238-242.

Kundu P.K. and J.S. Allen (1976). Some three-dimensional characteristics of the low-frequency current fluctuations near the Oregon Coast. *J. Phys. Oceanogr.* 6, 181-199.

Lacombe H. and P. Tchernia (1972a). Le problème de la formation des eaux marines profondes. Déroulement du phénomène en Méditerranée nord occidentale par hiver très froid (janvier-mars 1963). *Ann. Inst. Océanogr. XL, XIII*, 1, 75-110.

Lacombe H. and P. Tchernia (1972b). Caractères hydrologiques et circulation des eaux en Méditerranée. In: The Mediterranean Sea, D. J. Stanley ed. Dowden Hutchinson and Ross, Strousberg, 25-36.

López-Garcia M.J., C. Millot, J. Font and E. Garcia-Ladona (1994). Surface circulation variability in the Balearic Basin. *J. Geophys. Res.* 99, C2, 3285-3296.

Madec G., M. Crépon and M. Chartier (1991). The effect of the thermohaline forcing variability on deep water formation in the western Mediterranean Sea: a high-resolution three-dimensional numerical study. *Dyn. Atmos. Oceans* **15**, 35, 301-332.

MEDOC Group (1970). Observation of formation of deep water in the northwestern Mediterranean Sea. *Nature* **227**, 1037-1040.

Millot C. (1987a). Circulation in the western Mediterranean Sea. *Oceanologica Acta* **10**, 2, 143-149.

Millot C. (1987b). The structure of mesoscale phenomena in the Ligurian Sea inferred from the DYOME experiment. *Annales Geophysicae* **5B**, 1, 21-30.

Millot C. (1991). Mesoscale and seasonal variabilities of the circulation in the western Mediterranean. *Dyn. Atmos. Oceans* **15**, 35, 170-214.

Millot C. (1994). Models and data: a synergetic approach in the western Mediterranean Sea. P. Malanotte-Rizzoli and A.R. Robinson eds. Ocean Processes in Climate Dynamics: Global and Mediterranean Examples, 407-425.

Programme de Recherche International en Méditerranée Occidentale (PRIMO), Preparatory document on the development of PRIMO, an International Research Programme in the western Mediterranean, Publ. IOC/INF-772 UNESCO, Paris, 1989.

PRIMO document, (1991). Action plan of the International Research Programme in the western Mediterranean, Publ. IOC/INF-853 UNESCO, Paris.

Roberts J. and T.D. Roberts (1978). Use of the Butterworth low-pass filter for oceanographic data. *J. Phys. Oceanogr.* **83**, 5510-5514.

Sammari C., C. Millot and L. Prieur (1995). Some aspects of the seasonal and mesoscale variabilities of the Northern Current inferred from the PROLIG-2 and PROS-6 experiments. *Deep Sea Res.* In press.

Schott F. and K.D. Leaman (1991). Observations with moored Acoustic Doppler Current Profilers in the convection regime in the Golfe du Lion. *J. Phys. Oceanogr.* **21**, 4, 558-574.

Sciremammano F.Jr. (1979). A suggestion for the presentation of correlations and their signifiance levels. *J. Phys. Oceanogr.* **9**, 1273-1276.

Taupier-Letage I. and C. Millot (1986). General hydrodynamical features in the Ligurian Sea inferred from the DYOME experiment. *Oceanologica Acta* **9**, 119-131.

Ventsel H. (1973). Théorie des probabilités. MIR, 335 p.

Wallace J.M. and R.E. Dickinson (1972). Empirical orthogonal representation of the time series in the frequency domain. Part I. Theoretical consideration. *J. Appl. Meteo.* **11**, 887-892.